The LINNEAN SOCIETY of London ZOOLOGICAL Journal of the Linnean Society

Zoological Journal of the Linnean Society, 2016, **176**, 182–206. With 19 figures

Revision of the cranial anatomy and phylogenetic relationships of the Eocene minute boas *Messelophis variatus* and *Messelophis ermannorum* (Serpentes, Booidea)

AGUSTÍN SCANFERLA[1]*, KRISTER T. SMITH[2] and STEPHAN F. K. SCHAAL[2]

[1]*CONICET, Instituto de Bio y Geociencias del NOA (IBIGEO), 9 de Julio N° 14 (4405), Rosario de Lerma, Salta, Argentina*
[2]*Department of Palaeoanthropology and Messel Research, Senckenberg Research Institute, Senckenberganlage 25, 60325 Frankfurt am Main, Germany*

Received 12 March 2015; revised 16 May 2015; accepted for publication28 May 2015

We provide a detailed anatomical description of the skull of the fossil minute boas *Messelophis variatus* Baszio, 2004 and *Messelophis ermannorum* Schaal & Baszio, 2004 from the Middle Eocene Messel Formation (Germany), as well as a cladistic analysis to infer their phylogenetic relationships. Reanalysis of new and known specimens of both species demonstrates previously unrecognized anatomical characters in the skull of these fossil snakes. Both morphological and combined (morphology plus DNA) analyses place both species of *Messelophis* within a clade composed of boine, ungaliophiine, and erycine taxa. Cranial features that support this systematic arrangement include a well-developed medial foot process of the prefrontal, an expanded lateral flange of the prefrontal, and a well-developed surangular crest of the compound bone, among others. As a result of the incompleteness of some crucial cranial regions, such as the basicranium, their exact relationships within this clade are currently unresolved. *Messelophis* species display several contrasting traits that greatly exceed the morphological disparity found among extant genera of snakes. This cranial and postcranial anatomical variation between *M. variatus* and *M. ermannorum* demonstrates that this last species should be allocated to a new genus. ***Rieppelophis* gen. nov.** is therefore erected for the species ***Rieppelophis ermannorum* comb. nov.**

doi: 10.1111/zoj.12300

ADDITIONAL KEYWORDS: anatomical description – Messel formation – *Messelophis* – middle eocene – phylogeny – ***Rieppelophis* gen. nov.**

INTRODUCTION

The Messel Pit *Konservatlagerstätte*, near Darmstadt, Germany, is a UNESCO World Heritage site renowned for its exceptionally preserved fossil specimens. Methodical excavations at this site since 1975 have led to the identification of 138 vertebrate species (Morlo *et al*., 2004), including fishes, frogs, reptiles (crocodylians, turtles, lizards, and snakes), birds, and mammals that inhabited a small lake basin, under a warm, humid environment (Grein *et al*., 2011; Lenz, Wilde & Riegel, 2011). The Middle Messel Formation, from which all vertebrate specimens come, was recently dated to approximately 47.4–48.3 Mya, based on the astronomical tuning of pollen abundance profiles and revised $^{40}Ar/^{39}Ar$ dating of the phreatomagnatic eruption that produced the Messel crater (Lenz *et al*., 2015). Overall, several processes have served to preserve even the hair, feathers, 'skin shadows', wing membranes, stomach, and intestinal contents of some species, and even insect scale colouring, providing evidence for the feeding habits, ecology, and environment of the Eocene flora and fauna

*Corresponding author.
E-mail: agustin_scanferla@yahoo.com.ar

(Wuttke, 1983; Schaal & Ziegler, 1992; Vinther *et al*., 2010; McNamara *et al*., 2011; Smith & Wuttke, 2012).

Among the squamate species recovered in this fossil site, there are a large number of skeletons of different snake taxa, three of which were described as new species. All of them are booids, a group that was virtually extirpated from central and northern Europe by the Late Miocene (Szyndlar & Rage, 2003; Rage & Szyndlar, 2005). The first species is *Palaeopython fischeri* Schaal, 2004, described as a large booid with uncertain affinities within this clade (Schaal, 2004). The other two species are both very small, with maximum total lengths of about 40 cm, and the new genus *Messelophis* was erected by Baszio (2004) to accommodate them. The type species is *Messelophis variatus* Baszio, 2004, with one referred species *Messelophis ermannorum* Schaal & Baszio, 2004. These very small snakes (no more than 40 cm in length) were mainly diagnosed on the basis of their vertebral morphology. The original descriptions also briefly treated the skull anatomy of the two species, and their affinities were suggested to lie with the phylogenetically distant groups Tropidophiidae and Erycinae (Baszio, 2004; Schaal & Baszio, 2004). This conclusion was based mainly on comparisons of anatomical traits of the vertebrae, rather than a formal phylogenetic analysis.

The vast majority of snake fossils are isolated vertebrae with limited phylogenetically informative characters. The completeness of the Messel snakes makes these specimens highly relevant to understanding the phylogenetic relationships and early evolution of macrostomatan snakes; however, no detailed description or analysis of these exceptional forms has appeared since the original descriptions, and their anatomy and phyletic relationships consequently remain currently poorly understood. In the past decade, microcomputed tomography (mCT) technology and accessibility have advanced dramatically, allowing previously unobservable parts of the fossils to be studied. In this paper we redescribe the skull anatomy of these important fossil snakes, and for the first time present a detailed analysis of their phylogenetic relationships.

MATERIAL AND METHODS

The study presented herein is based on the analysis of new and previously known specimens of *Messelophis* deposited in the Messel collection of the Senckenberg Research Institute in Frankfurt am Main (SMF ME) and the Messel collection of the Hessisches Landesmuseum in Darmstadt (HLMD-Me), and a new specimen housed in the American Museum of Natural History (AMNH). All specimens were completely extricated from the matrix and embedded in epoxy plates; some vertebrae had also previously been extracted from the specimens in order to better document vertebral morphology. Because of the transparent nature of the epoxy resin plate, we could study the embedded side of some specimens of *M. variatus* (e.g. SMF ME 1828 a+b) without mCT scans in order to reveal new and noteworthy anatomical information.

We rely principally on the paratype specimen HLMD-Me 7915, the most nearly complete and practically undistorted specimen of these small snakes. To reveal some important parts of the ventral skull covered by oil shale, this specimen was scanned at the high-resolution X-ray CT (HRXCT) facility of the Wolfgang Pfeiffer Stiftung at the Technische Hochschule in Deggendorf, Germany. The reconstructions have an in-plane resolution of 12.2 μm per pixel. The image processing was performed with VGStudio MAX 2.2 (Volume Graphics, Heidelberg, Germany). The density contrast between bone and the epoxy plate was high and permitted digital 'preparation' of the specimen, rendering the matrix completely transparent.

RESULTS

NEW ANATOMICAL OBSERVATIONS OF THE SKULL OF *MESSELOPHIS VARIATUS*

Premaxilla

As was pointed out by Baszio (2004: fig. 11), specimen SMF ME 2379 of *M. variatus* exhibits a toothed premaxilla, a condition shared with *Anilius* and basal macrostomatans, such as *Xenopeltis*, *Loxocemus*, and pythonines (Smith, Bellairs & Miles, 1953). The premaxilla of *M. variatus* also has a well-developed ascending process (Fig. 2). This structure, which is present in boine snakes *Exiliboa* and *Ungaliophis* but is absent in tropidophiids, is clearly visible in the snout region of the holotype specimen SMF ME 1828 a+b and in AMNH FARB 30650. The nasal bones clasp the dorsal tip of this process in the former specimen, in a way similar to the condition in boines such as *Boa constrictor* Linnaeus, 1758. Also, Baszio (2004) briefly mentioned the presence of an articular facet on the premaxilla that contacts the anterior tip of the maxilla. Although he did not specify the exact position and morphology of the articular facet, we interpret that this structure would have to be located in the posterior edge or at the tip of the transverse process of the premaxilla, as occurs in lizards. An articular contact between premaxilla and maxilla is a rare condition among snakes, documented only in the fossil 'madtsoiid' *Yurlunggur* (Scanlon, 2006; Fig. 3C) and uropeltids (Olori & Bell, 2012; Fig. 3D). In these snakes there is a well-defined facet at the tip of the transverse process of the premaxilla and a corresponding facet at the anterior tip of the maxilla (Fig. 3). On the right side of the holotype specimen (Fig. 3A), it is possible to observe that the tip of the transverse process of the premaxilla

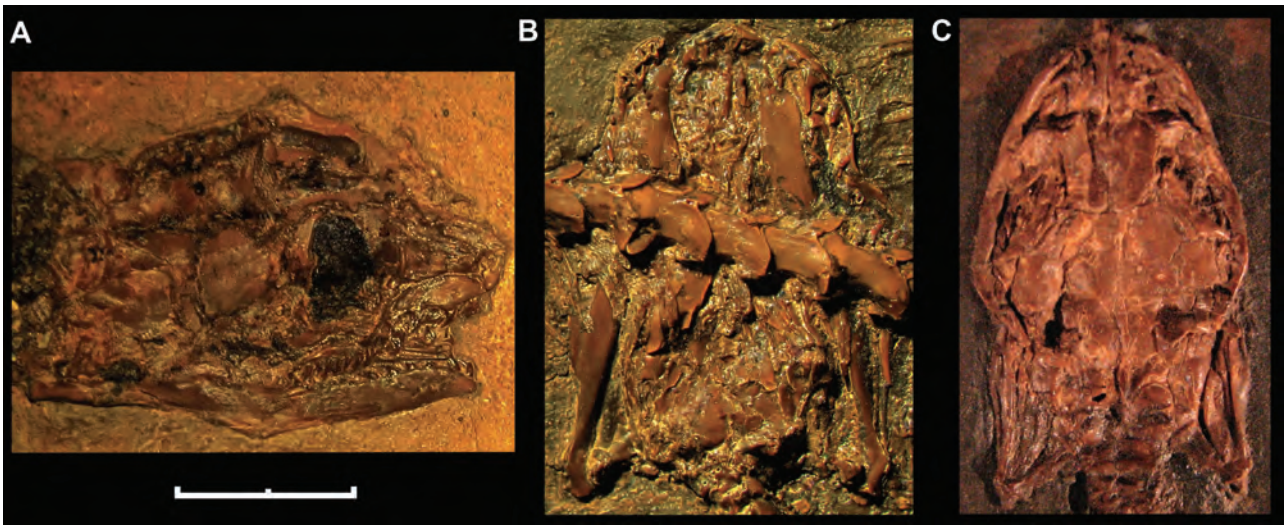

Figure 1. Most complete and informative preserved skulls of *Messelophis variatus* from the Middle Eocene Messel Formation, Germany: A, holotype specimen SMF ME 1828 a+b, in right lateral view; B, ventral view of the skull of paratype specimen SMF ME 2379, partially covered by mid-trunk vertebrae; C, dorsal view of the skull of a new undescribed specimen AMNH FARB 30650. Scale bar: 5 mm.

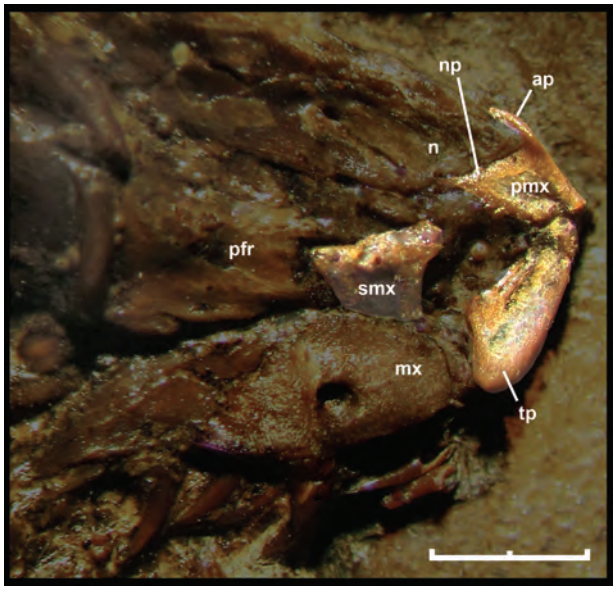

Figure 2. Lateral right view of the snout of *Messelophis variatus* (SMF ME 1828 a+b). Scale bar: 1 mm. Abbreviations: ap, ascending process of the premaxilla; mx, right maxilla; n, right nasal; np, nasal process of premaxilla; prf, prefrontal; pmx, premaxilla; smx, lateral vertical flange of septomaxilla; tp, transverse process of premaxilla.

is located close to the anterior tip of the maxilla, but is not in contact with it. Also, there are no signs of an articular facet either on the premaxilla or on the maxilla in any specimens of this species examined. In fact, the transverse process terminates in a somewhat rounded tip, as in most extant snakes (Fig. 3B). Thus, we consider that *M. variatus* lacks an articular contact between the premaxilla and the maxilla (contra Baszio, 2004). The possible occurrence of vomerine processes cannot be evaluated because of poor preservation.

Septomaxilla

The holotype preserves a small fragment of the right septomaxilla in lateral view (Fig. 2), located above the anterior portion of the right maxilla. This fragment corresponds to the lateral vertical flange, which exhibits the typical alethinophidian condition of a dorsal laminar projection with a broad base. In its anterodorsal corner, this flange possesses a small anteriorly directed projection as in a number of macrostomatans like *Python*. As a result of the fragmentary condition of the lateral vertical flange, it could not be determined whether the posterior dorsal process is broken or absent.

Prefrontal

AMNH FARB 30650 and SMF ME 1828 a+b provide novel information about the morphology of this circumorbital bone (Fig. 4A). Despite the incompleteness of the anterior region of preserved prefrontals in both specimens, it can be inferred that both lateral and dorsal laminae were expanded, as in most booids; however, the dorsal lappet of pythonines and boines is not present. As in most macrostomatans, the prefrontal of *M. variatus* seems to retain only a posterior contact with the dorsal surface of the maxilla through a tongue-like lateral foot process. Dorsal to this structure is a conspicuous outer orbital lobe that

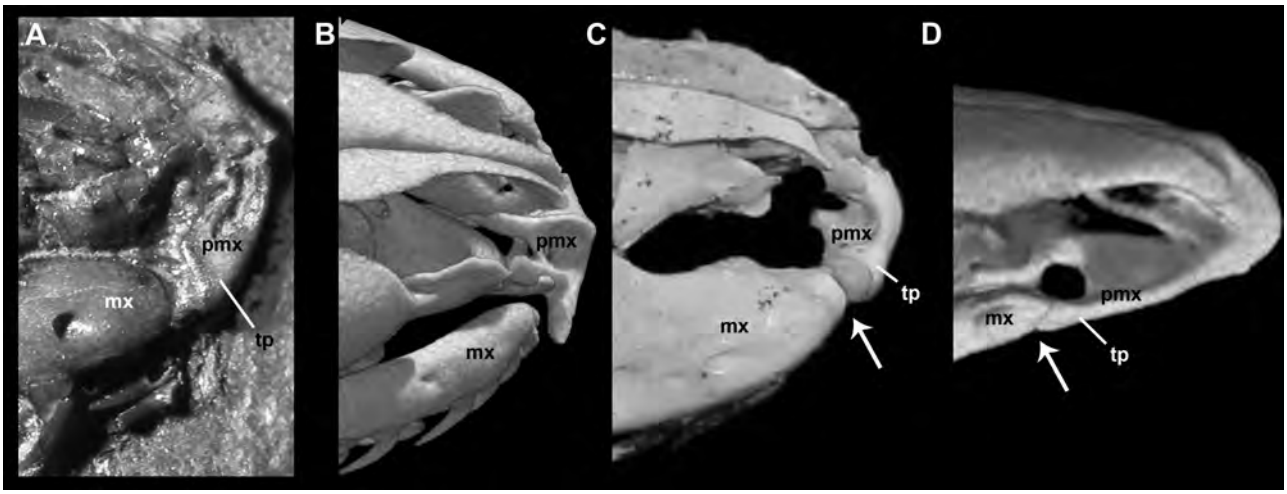

Figure 3. Dorsolateral view of the rostral region of *Messelophis variatus* (A), *Tropidophis haetianus* (B), *Yurlunggur* sp. (C), and *Uropeltis woodmasoni* (D). Arrows indicate the contact area between the transverse process of the premaxilla and the anterior tip of maxilla. Not drawn to scale. Abbreviations: mx, maxilla; pmx, premaxilla; tp, transverse process of premaxilla.

reaches the dorsal region of the prefrontal. This lobe is found also in boines and erycines in different degrees of development (Fig. 4D). The medial foot process is a remarkably long finger-like structure, approaching the development observed in boines and erycines. Between these processes is a deep notch that received the lacrimal duct; in the fossil species, as in boines, erycines, *Ungaliophis*, and *Exiliboa*, it opens ventrally.

Postorbital

Although this bone is present in most specimens of *M. variatus*, the right postorbital of AMNH FARB 30650 is preserved practically undistorted, located close to its original anatomical position (Fig. 4B). In dorsal view, this bone is characterized by a long unforked dorsal region that lies upon a narrow shelf of the parietal and makes contact with the posterior part of the supraorbital margin of the frontal. The dorsal portion, which contacts the postorbital process of the parietal, is strongly anteriorly expanded and forms a lamina. This expansion is also observed in boines and pythonines. In contrast, the ventral portion is slender. The length and orientation observed in examined specimens suggest that the postorbital probably contacted a ventral element (maxilla or ectopterygoid), as was pointed out by Baszio (2004). The inferred morphology is similar to that present in *Eryx* and *Ungaliophis*, but in those snakes the region that contacts with the postorbital process of the parietal is not expanded.

Ectopterygoid

The morphology of this bone in *M. variatus* is best seen in AMNH FARB 30650 (Fig. 4C) and the embedded side of SMF ME 958b. Both ectopterygoids are present in AMNH FARB 30650 in articulation with maxillae. The exact length of the ectopterygoid cannot be determined because the posterior part seems to be broken; however, it is clear that this bone has a well-developed shaft without signs of reduction, unlike in small booids like *Lichanura* or *Ungaliophis* (Fig. 4F). The ectopterygoid shaft exhibits a slightly curved lateral edge, as in numerous macrostomatans. The right ectopterygoid of AMNH FARB 30650 preserves the maxillary process, which bears a small anteromedial prong (partially covered by an unidentified fragment of bone) and an anterolateral prong, which between them bound a small notch. This morphology, which is also seen in boines, ungaliophiines, and pythonids, contrasts with that in erycines and tropidophiids, where the anterior end of the ectopterygoid is unforked.

Pterygoid

A small fragment identified as the palatine ramus of the pterygoid can be observed in the embedded side of SMF ME 1828 a+b. Because of its fragmentary nature, we only recognize the presence of the base of three small teeth. Additionally, AMNH FARB 30650 bears both quadrate rami of the pterygoid bones in dorsal view (Fig. 1C). The preserved portion of the right pterygoid clearly exhibits a blade-like structure, although the state of preservation prohibits the identification of other important features like a dorsal keel, which is present in some booids.

Parietal

Like most braincase elements of *M. variatus*, the parietal is strongly crushed in all specimens examined;

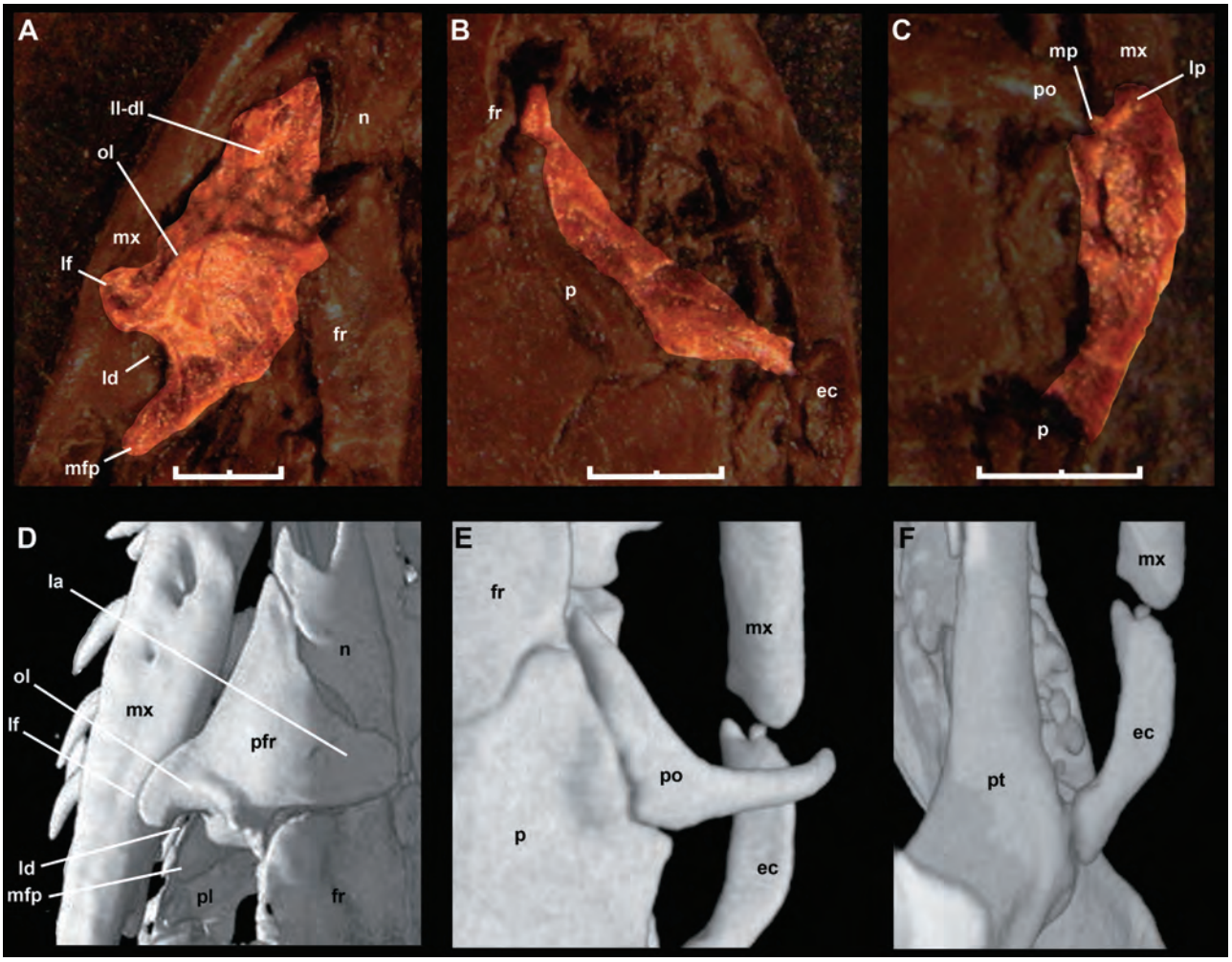

Figure 4. Dorsal view of left prefrontal (A), right postorbital (B), and right ectopterygoid of *Messelophis variatus* (AMNH FARB 30650). D, dorsolateral view of left preorbital region of *Boa constrictor* based on HRXCT data. E, dorsal view of right postorbital region of *Ungaliophis continentalis* based on HRXCT data. F, dorsal view of the right palatomaxillary arch of *Ungaliophis continentalis* (three-dimensional cutaway view based on HRXCT data). For *Messelophis* panels, scale bars equal 1 mm, the others are not to scale. Abbreviations: ec, ectopterygoid; fr, frontal; la, dorsal lappet; ld, lacrimal duct; lf, lateral foot process; ll, lateral lamina of prefrontal; ll-dl, undifferentiated lateral and dorsal lamina of prefrontal; lp, anterolateral prong; mfp, medial foot process; mp, anteromedial prong; mx, maxilla; n, nasal; ol, outer orbital lobe; p, parietal; pfr, prefrontal; pl, palatine; po, postorbital; pt, pterygoid.

however, specimen AMNH FARB 30650 adds further anatomical information about the dorsal aspect of this bone (Fig. 5). The anterior margin that contacts with frontal bones is concave because of the presence of small, anteriorly directed supraorbital processes, a feature that is also observed in small booids like *Ungaliophis*. In dorsal view, it is possible to recognize a weakly defined parietal table, which is also present in small booids such as *Exiliboa*, *Ungaliophis*, erycines (except *Eryx*), and derived macrostomatans. As pointed out by Baszio (2004), the parietal bears a sagittal crest on the posterior third. This crest continues backwards as a pointed posterior process, as in erycines and boines, concealing the mid-sagittal part of the supraoccipital bone. As a result of the displacement of the postorbital from its articular position, it is possible to observe a small postorbital process in the right side of the parietal of AMNH FARB 30650 and SMF ME 1828 a+b. Also, the parietal develops a shelf that extends from the anterior end of the supraorbital process to the postorbital process.

Prootic

A thorough examination of the embedded side of SMF ME 1828 a+b gives a satisfactory view of the (left) lateral side of the braincase of *M. variatus* (Fig. 6A).

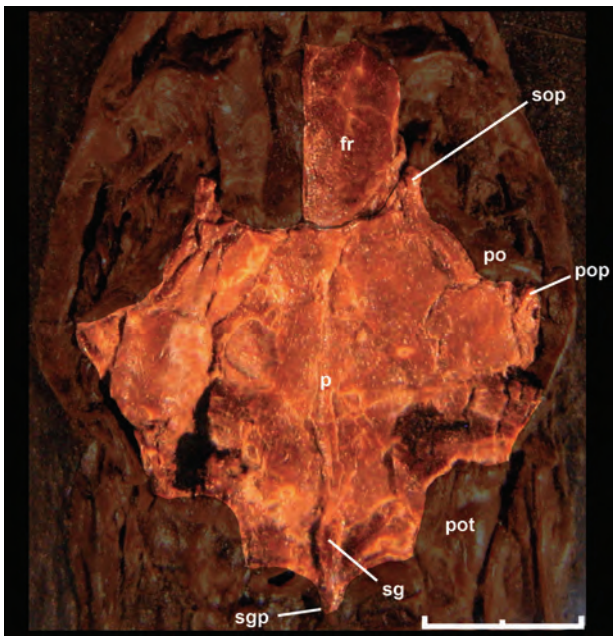

Figure 5. Dorsal view of skull roof of *Messelophis variatus* (AMNH FARB 30650). Scale bar equals 2 mm. Abbreviations: fr, frontal; p, parietal; po, postorbital; pot, prootic; pop, postorbital process; sg, sagittal crest; sgp; sagittal process; sop, supraorbital process.

The prootic is similar to that of small booid snakes such as *Lichanura* (Fig. 6C) and *Ungaliophis* (Fig. 6D). The anterior (V2) trigeminal foramen is delimited anteriorly by the parietal and the prootic because of the weak development of the dorsal and ventral anterior processes of the prootic. In tropidophiids (Fig. 6B) and most booids, in contrast, these processes in adult specimens are in contact anterior to the anterior (V2) trigeminal foramen, enclosing it (Scanferla & Bhullar, 2014). The laterosphenoid is present as a broad strip of bone that separates the anterior and posterior parts of the trigeminal chamber. Ventral to the anterior end of this bone is a small foramen that topologically corresponds to the foramen for the re-entry of the cid nerve described by Rieppel (1979) in several macrostomatans. At the ventral region of the posterior trigeminal chamber is a small foramen that corresponds with the hyomandibular branch of the facial nerve (VII). In contrast to small booids, the fenestra ovalis is moderate in size. Additionally, the crista prootica is weakly developed and exposes part of the stapedial footplate.

Otooccipital

Parts of the left otoocipital can be seen in the embedded side of SMF ME 1828 a+b (Fig. 6A); however, only the crista interfenestralis and the apertura lateralis recessus scalae tympani are recognizable. As in most macrostomatans, the crista interfenestralis, which is interposed between the lateral aperture of the recessus scalae tympani and the fenestra ovalis, forms an individualized component in the ventral region of the juxtastapedial recess.

Stapes

The left stapes is preserved and visible in articulation in SMF ME 1828 a+b (Fig. 6A). The stapedial shaft is present but partially covered by the quadrate shaft. The observable portion of this structure indicates that its length is much greater than the diameter of the footplate, as in most macrostomatans. The shaft extends posterodorsally to attach to the cephalic condyle or the quadrate shaft. *Messelophis variatus* has a small footplate, similar to that of large booids, but in contrast to the typical condition in small-sized macrostomatans, which exhibit a large footplate with respect to the size of the neurocranium (e.g. *Lichanura*; see Fig. 6C). Furthermore, the footplate in *M. variatus* is not covered by any component of the crista circumfenestralis; however, we cannot rule out the possibility that this condition is a product of the compression suffered by the holotype specimen.

Supratemporal

The embedded side of SMF ME 1828 a+b also offers a lateral view of the left supratemporal in articulation (Fig. 6A). The former is flat bone and is applied to the dorsal surface of the prootic without the development of a distinct facet on the latter bone, and its posterior part articulates with the cephalic condyle of the quadrate. Although the articulation with the skull is surely slightly distorted, it is clear that the posterior end of the supratemporal does not surpass the posterior part of the neurocranium (i.e. a free-ending process was minute or absent). Although the posterior skull roof of specimen AMNH FARB 30650 is badly damaged, it can be inferred that supratemporals have the same short length as in the holotype specimen (Fig. 1C). Moreover, the articular relationship of the supratemporal with the quadrate and the skull roof in both specimens supports the (near) absence of a free-ending process, as is found in most small-sized booids like *Lichanura* (Fig. 6C). This interpretation contrasts with Baszio (2004), who described a slender supratemporal in the paratype specimen SMF ME 2379 and compared it with that in *Boa*, which has a long, free-ending process in adult specimens.

Lower jaw

Several relevant features of the lower jaw can be recognized in the embedded side of the holotype specimen SMF ME 1828 a+b and SMF ME 958b, which offer lateral and medial views of the right lower jaw and a lateral view of the right compound bone, respectively

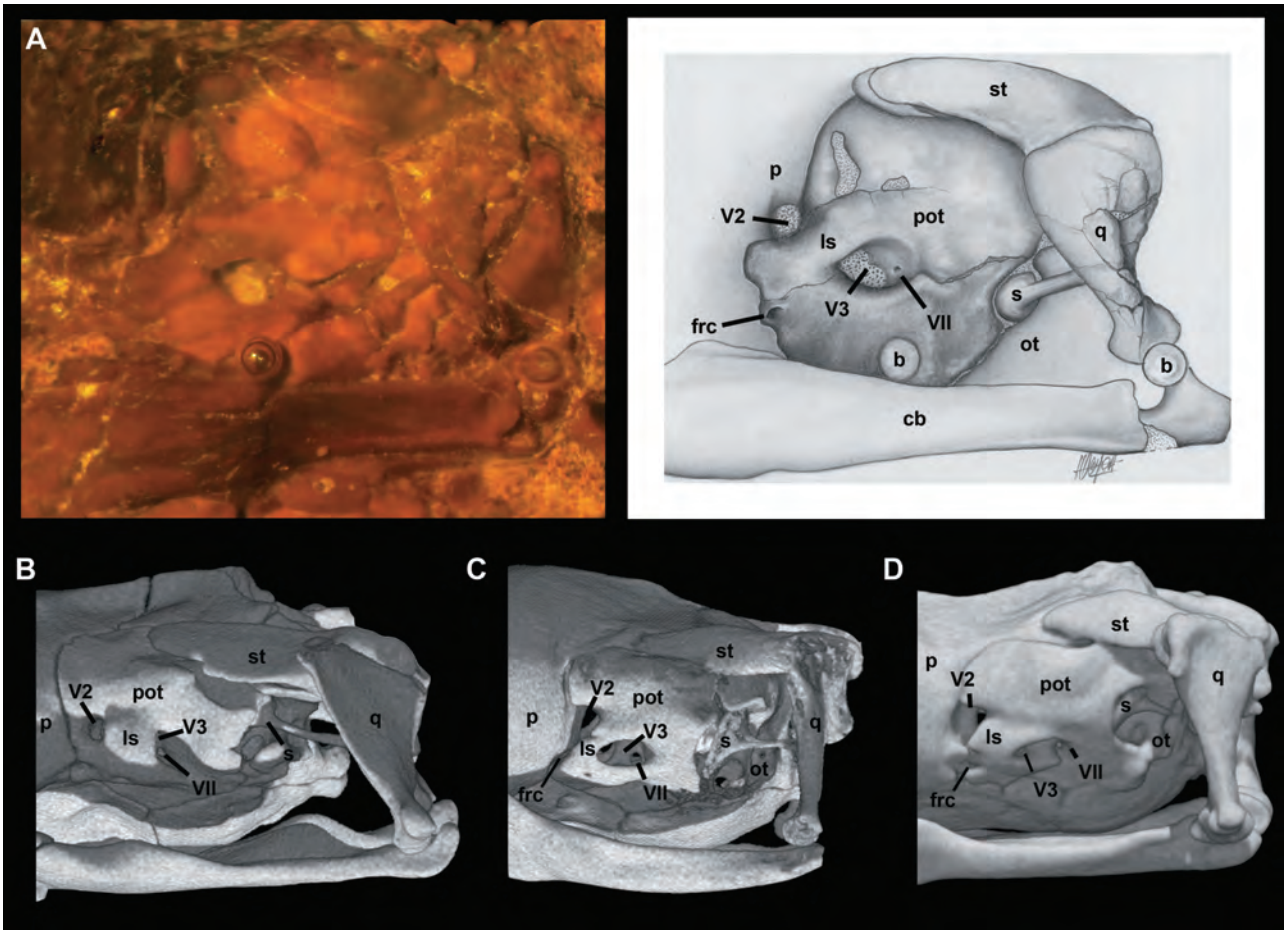

Figure 6. A, embedded side of the holotype specimen of *Messelophis variatus* (SMF ME 1828 a+b), with a left lateral view of the skull. Lateral views of the posterior part of the skulls of *Tropidophis haetianus* (B), *Lichanura trivirgata* (C), and *Exiliboa placata* (D). Abbreviations: b, bubble; cb, compound bone; frc, foramen for the re-entry of the cid nerve; ls, laterosphenoid; ot, otooccipital; p, parietal; pot, prootic; q, quadrate; s, stapes; st, supratemporal; V2, anterior trigeminal foramen; V3, posterior trigeminal foramen; VII, foramen for the passage of the facial nerve.

(Fig. 7). The lateral aspect of the dentary reveals a large mental foramen located at the fourth tooth position (Fig. 7A). Several teeth are visible in lateral view; they are recurved and somewhat slender. The medial view of SMF ME 1828 a+b shows a wide Meckelian groove that opens medially along its length (Fig. 7B). The splenial is long and somewhat narrow anteriorly; there is a long anterior process that tapers anteriorly to a pointed tip, thus closing the Meckelian groove ventromedially. Posteriorly the dorsal margin of the splenial is notched, forming an anterodorsal spine. The splenial and angular meet in an abutting contact, thus forming a well-developed intramandibular joint. The coronoid bone is present, but its dorsal portion is incomplete. This postdentary element is a sliver of bone applied to the medial side of the coronoid prominence of the compound bone. It shows a long anteroventral process that narrowly contacts the posterodorsal margin of the splenial, the medial side of the posterior region of the dentary, and the anterodorsal margin of the angular. The compound bone (Fig. 7C) exhibits a well-developed, asymmetrical surangular crest, the apex of which lies near the anterior end of the bone. Its dorsal margin forms a straight line from the coronoid prominence to the glenoid fossa. The anterior surangular foramen is situated at the base of the coronoid prominence. Posteriorly, the compound bone possesses a short and blunt retroarticular process.

Anatomical redescription of the skull of *Messelophis ermannorum*

Premaxilla

This bone is well preserved in HLMD-Me 7915 (Fig. 8, Fig. 9A, B). Schaal & Baszio (2004) stated that

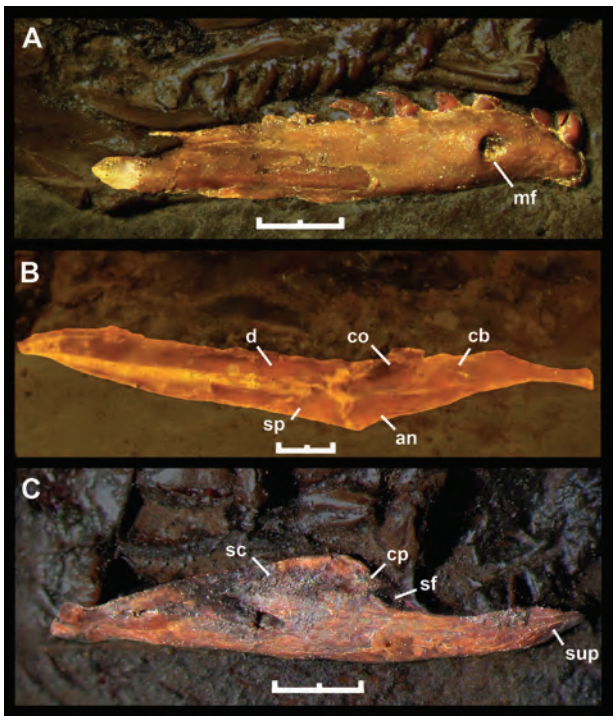

Figure 7. Lower jaw morphology of *Messelophis variatus*: A, lateral view of the right dentary of the holotype specimen SMF ME 1828 a+b; B, medial view of the right lower jaw in the embedded side of the specimen SMF ME 1828 a+b; C, lateral view of the right compound bone of specimen SMF ME 958 b. Scale bars: 1 mm. Abbreviations: an, angular, cb, compound bone; co, coronoid; d, dentary; mf, mental foramen; sc, surangular crest; sf, anterior surangular foramen; sp, splenial; sup, surangular process.

M. ermanorum has an edentulous premaxilla, a condition that strongly contrasts with respect to the toothed premaxilla of *M. variatus*. New mCT data of the specimen confirm that observation, revealing that the premaxilla of *M. ermannorum* lacks teeth and tooth positions. Another important difference between these forms is the shape of the transverse process, which is larger and more gracile in *M. ermannorum* than in *M. variatus*. As in *M. variatus* and boines, there is a well-developed ascending process, but its length cannot be ascertained because the distal end is broken. In ventral view, the premaxilla of *M. ermannorum* exhibits a conspicuous vomerine process. Although its morphology is difficult to determine because of the damage suffered by this specimen to its ventral side, it does not appear to be paired as in erycines.

Nasal

Both nasals are well preserved in HLMD-Me 7915, only slightly displaced from their anatomical position (Fig. 9C, D). Anteriorly, the dorsal (horizontal) lamina tapers to a pointed tip, as in *M. variatus* (Baszio, 2004), thus forming a slightly concave lateral margin. Laterally, the lamina curves downwards, and part of the lateral margin inserts into a small notch in the dorsal edge of the dorsal lamina of prefrontal (Fig. 9C). Moreover, the ventral view of the left nasal (Fig. 9D) shows that the distal terminus of the dorsal lamina established contact with the dorsal lamina of the prefrontal, as occurs in some boines such as *Eunectes* and *Boa* (see Fig. 4D). The vertical (medial) nasal flange is well developed, and reaches its maximum extent in the area of contact with the premaxilla. Posteriorly, the vertical (medial) flange displays a distinct articular surface, which would have been in contact with the medial frontal pillar, as is typical of the booid nasofrontal joint (Rieppel, 2007).

Septomaxilla

HLMD-Me 7915 preserves a portion of the right septomaxilla (Fig. 9E, F). As in most non-caenophidian alethinophidian snakes, the lateral vertical flange exhibits a broad base and a well-developed posterior dorsal process. Usually, this posterior process is relatively large and slender, but *M. ermannorum* exhibits a remarkably expanded posterior dorsal process. Among extant snakes, only *Exiliboa* approaches this condition. In ventral view (Fig. 9F), it is possible to distinguish the contribution of the septomaxilla with the anterior wall of the cavity that houses Jacobson's organ.

Prefrontal

Both prefrontals are preserved in HLMD-Me 7915 (Fig. 10). This bone resembles the typical booid condition previously observed in *M. variatus*. The lateral aspect of both prefrontals exhibits an expanded lateral lamina, as in most booids, suggesting that this structure covered the nasal gland laterally. The dorsal margin of this lamina exhibits a notch that contacts part of the lateral edge of the dorsal (horizontal) lamina of nasal, as previously mentioned. Despite its resemblance to boines and pythonines, the prefrontal lacks the dorsal lappet typically present in these groups. The lateral aspect of the prefrontal shows a conspicuous outer orbital lobe, as in *M. variatus* and many booids. There is a well-developed lateral foot process, which constitutes the only region of the ventrolateral margin of the prefrontal that establishes contact with the dorsal surface of the maxilla. The medial foot process is strong, although it is relatively shorter than the same structure in *M. variatus*. As in *M. variatus*, boines, erycines, and ungaliophiines, the lacrimal notch opens ventrally. We interpret the right prefrontal as being close to its natural position with respect to the maxilla (Fig. 10A). If this interpretation is correct, the medial foot process is in contact with the dorsal surface of the medial portion of the palatine process of the maxilla.

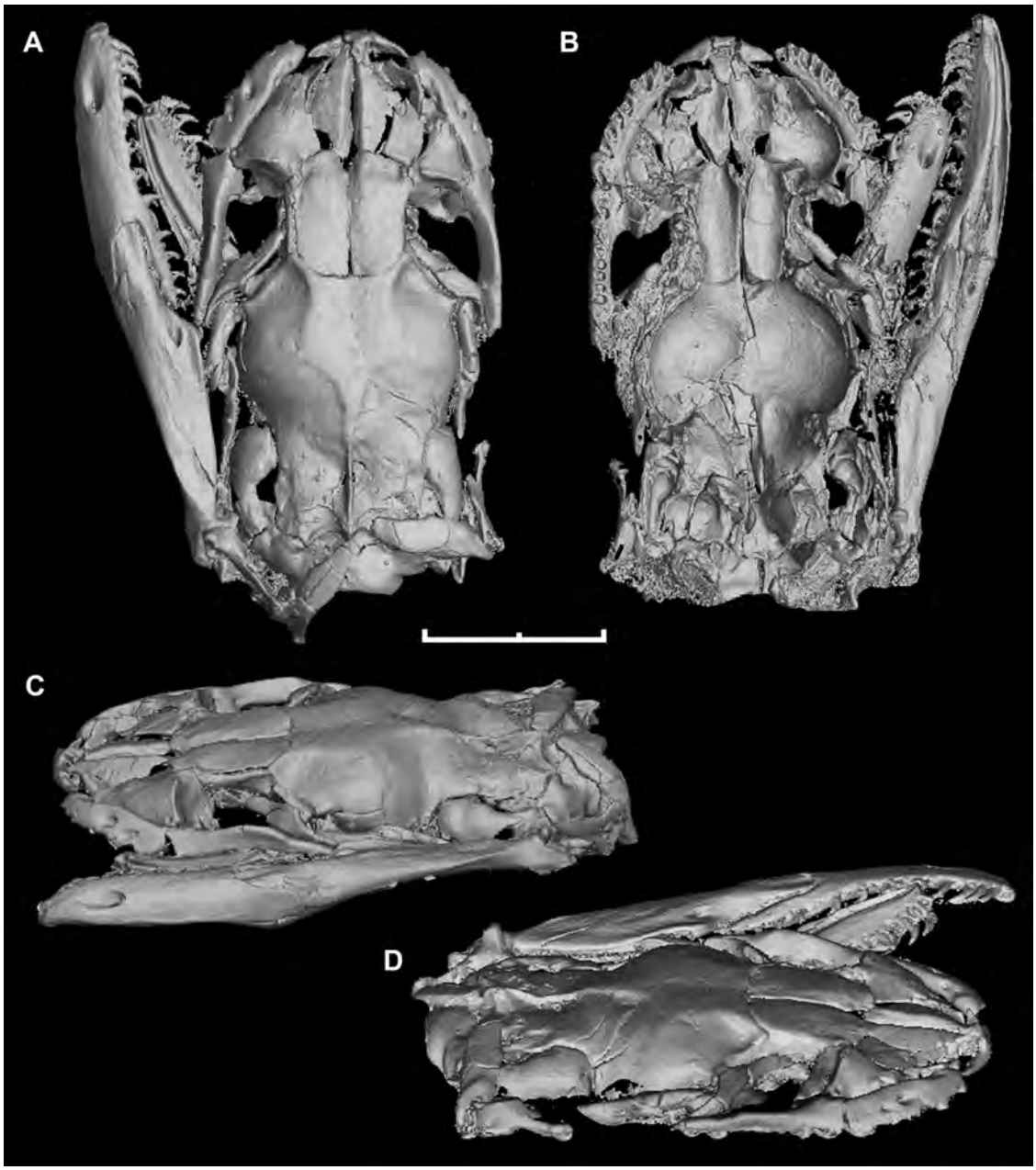

Figure 8. Three-dimensional reconstruction of the skull of the paratype specimen of *Messelophis ermannorum* (HLMD-Me 7915) based on HRXCT data in dorsal (A), ventral (B), left dorsolateral (C), and right dorsolateral (D) views. Scale bar: 5 mm.

This articular condition – characterized by the aforementioned relation plus a well-developed lateral foot process in contact with the dorsal surface of the maxilla – strongly resembles the boine prefrontal–maxilla articulation (compare with Fig. 4D).

Postorbital

Both postorbitals are present and undistorted in specimen HLMD-Me 7915 (Fig. 10). The morphology of this bone strongly resembles that of *M. variatus* described above. The unforked dorsal region is applied to the anterolateral corner of the parietal and the most posterior part of the supraorbital margin of the frontal. The slight displacement of the right postorbital demonstrates that this region articulates along a shelf modelled in the parietal bone. As in *M. variatus*, the dorsal portion of the bone is strongly anteriorly expanded and confers a laminar shape to this part of the postorbital.

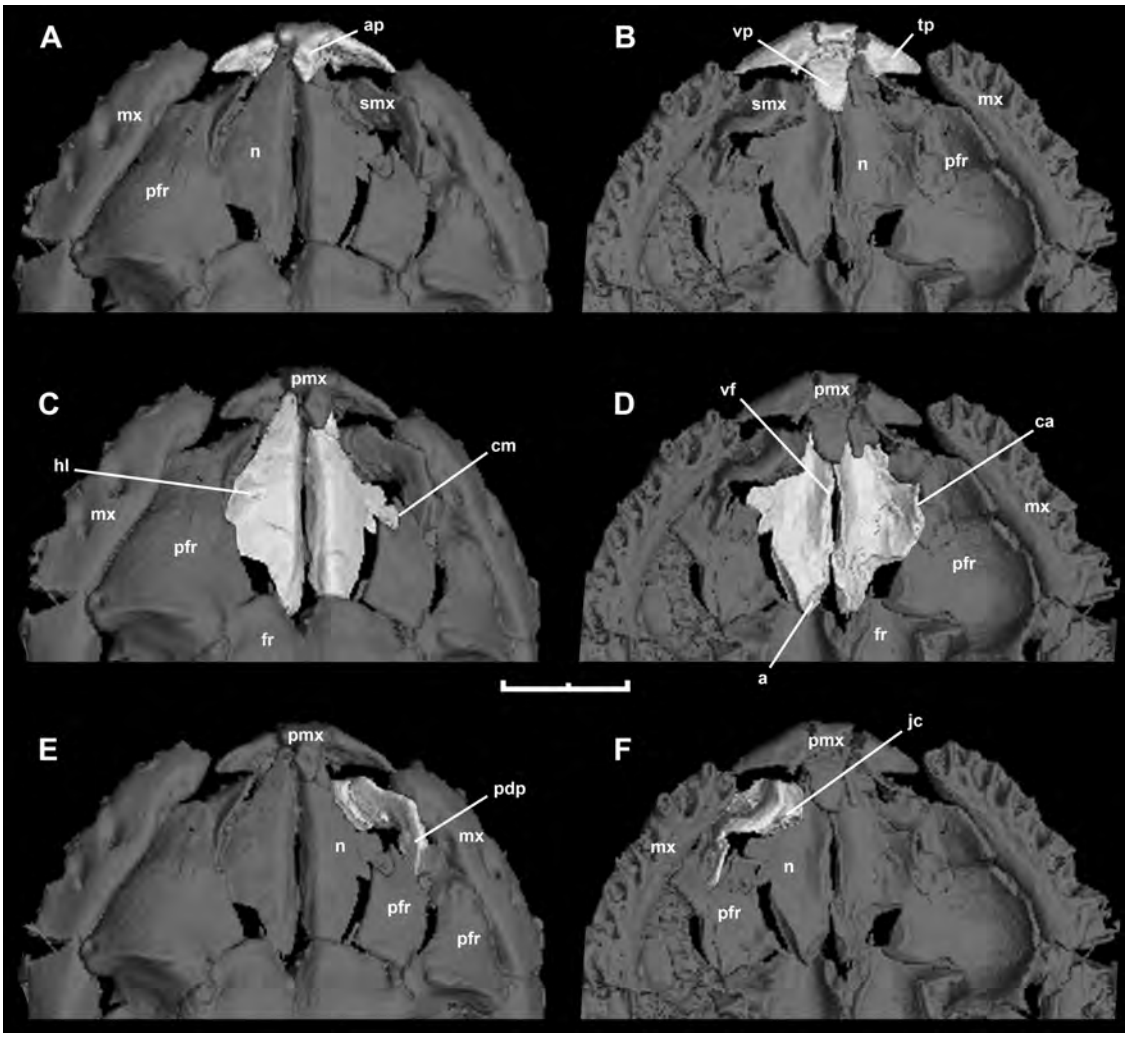

Figure 9. Three-dimensional reconstruction of rostral region of paratype specimen of *Messelophis ermannorum* based on HRXCT data: dorsal (A) and ventral (B) views of premaxilla; dorsal (C) and ventral (D) view of nasals; dorsal (E) and ventral (F) views of right septomaxilla. Scale bar: 2 mm. Abbreviations: a, articular area of the nasal with frontal; ap, ascending process of the premaxilla; ca, contact area with prefrontal; cm, contact margin of the nasal with prefrontal; fr, frontal; hl, dorsal (horizontal) lamina of nasal; jc, anterior wall of the cavity housing Jacobson's organ; mx, maxilla; n, nasal; pdp, posterior dorsal process of septomaxilla; pfr, prefrontal; pmx, premaxilla; smx, septomaxilla; tp, transverse process of premaxilla; vf, medial (vertical) flange of nasal; vp, vomerine process of premaxilla.

The ventral portion, located posterior to the orbit, is more slender than the dorsal portion; it curves posteroventrally and tapers distally. The ventral tip, which would have contacted the maxilla or ectopterygoid, lacks the foot-like shape present in most pythonines and boines.

Maxilla

Both maxillae are present and undistorted in HLMD-Me 7915 (Fig. 11), but only the right maxilla is well exposed. This bone is slender, and its anterior portion shows the distinct medial curvature seen in most booids. The posterior region is straight, and the region of contact with the ectopterygoid is lower and more delicately built. In lateral view, there are two labial foramina, the anterior larger than the posterior, located at the sixth and eighth tooth positions, respectively. This condition contrasts with the single labial foramen present in *M. variatus*, which is located more anteriorly (at the fourth tooth position). Schaal & Baszio (2004) identified on the basis of superficial examination the presence of 15 maxillary teeth; however, a ventral view obtained through CT reveals 22 ± 1 tooth positions. The teeth are mostly crushed or absent, with the exception of two teeth at the middle of the maxilla. The preserved bases of some anterior teeth and the size of tooth

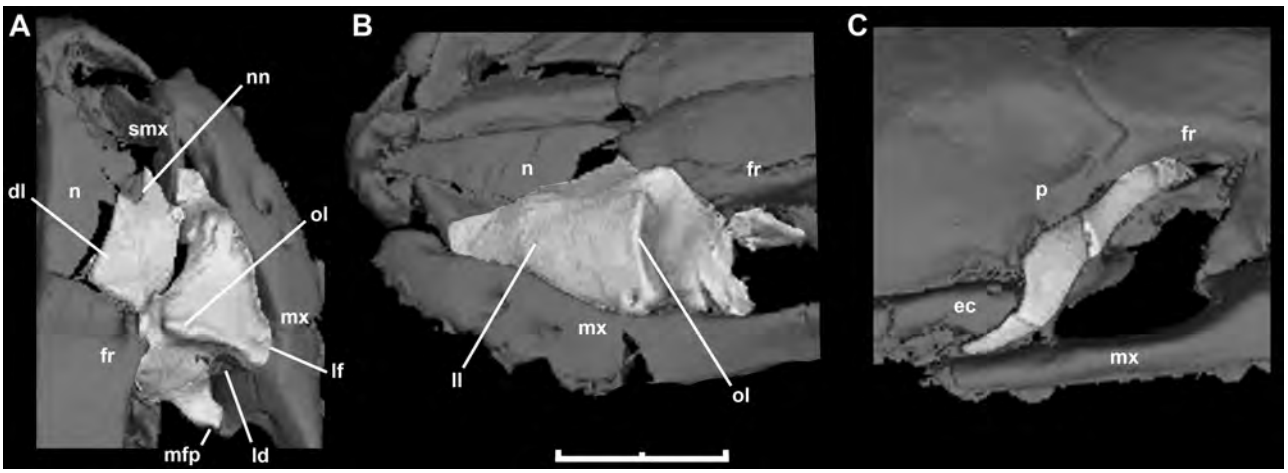

Figure 10. Three-dimensional reconstruction of the circumorbital bones of the paratype specimen of *Messelophis ermannorum* (HLMD-Me 7915) based on HRXCT data: A, right prefrontal in dorsal view; B, left prefrontal in lateral view, C, right postorbital in dorsolateral view. Scale bar: 2 mm. Abbreviations: dl, dorsal lamina of prefrontal; ec, ectopterygoid; fr, frontal; ld, lacrimal duct; lf, lateral foot process; ll, lateral lamina of prefrontal; mfp, medial foot process; mx, maxilla; n, nasal; nn, nasal notch; ol, outer orbital lobe; smx, septomaxilla.

positions indicates that there is a strong anteroposterior decrease in tooth size, similar to the condition in most booids. The bases of the teeth are robust and rounded, without signs of folded enamel or dentine. Preserved entire teeth are conical, recurved, and pointed. The palatine process is located at the middle of the bone and posteromedially oriented. At the posterolateral corner of this process there is a small foramen and a shallow groove corresponding to the superior alveolar foramen and its groove. *Messelophis ermannorum* lacks the ectopterygoid process at the posterior end of the maxilla, in contrast with derived macrostomatans. Posteriorly, there is a shelf onto which the ectopterygoid articulated. The foramen for the superior alveolar nerve pierces the posterodorsal margin of the palatine process close to its junction with the main body of the maxilla.

Ectopterygoid

The mCT reconstruction provides satisfactory dorsal and ventral views of both ectopterygoids of HLMD-Me 7915 (Fig. 11C, D). The ectopterygoid shaft is robust and straight, in contrast to the weakly curved shaft previously described for *M. variatus*. Anteriorly is a forked maxillary process that overlapped the posterior end of the maxilla. The anterolateral prong of the maxillary process is somewhat bulbous and longer than the anteromedial prong, which would have extended to the level of the ventral tip of the postorbital. The pterygoid process of the ectopterygoid is barely differentiated from the shaft. In dorsal view (Fig. 11C) the medial region of this process exhibits a gently convex surface that is in close proximity to the concave articular surface on the lateral margin of the pterygoid. Furthermore, the right ectopterygoid shows the same morphology and relationship with the right pterygoid (Fig. 11D, E). This kind of articular relationship between ectopterygoid and pterygoid bones resembles the condition present in erycines, boines, and *Ungaliophis*, where a laterally positioned well-delimited concave surface receives the posteriormost medial (convex) surface of the pterygoid process of the ectopterygoid.

Pterygoid

A small portion each of the left and right pterygoids is present in HLMD-Me 7915 (Fig. 11). The right pterygoid fragment shows a laterally positioned concave area that received the ectopterygoid (Fig. 11E). The same articular area is seen in the dorsal view of the preserved portion of the left pterygoid (Fig. 11C). Additionally, the left pterygoid fragment preserves part of the quadrate ramus (Fig. 11F), which exhibits a laminar conformation, as in most macrostomatans.

Palatine

The right palatine bone is preserved in SMF ME 11426 only, yet is slightly compressed and still articulated with a small fragment of the palatine ramus of the pterygoid (Fig. 12). Despite the poor state of preservation, it is possible to observe some relevant traits. Most of the palatine is composed of a prominent and toothed anterior (dentigerous) process that reveals at least six tooth positions, most of these occupied by the base of teeth only. The anteriormost tooth is the best preserved of the palatine dentition, showing that palatine teeth were similar in size to the maxillary teeth,

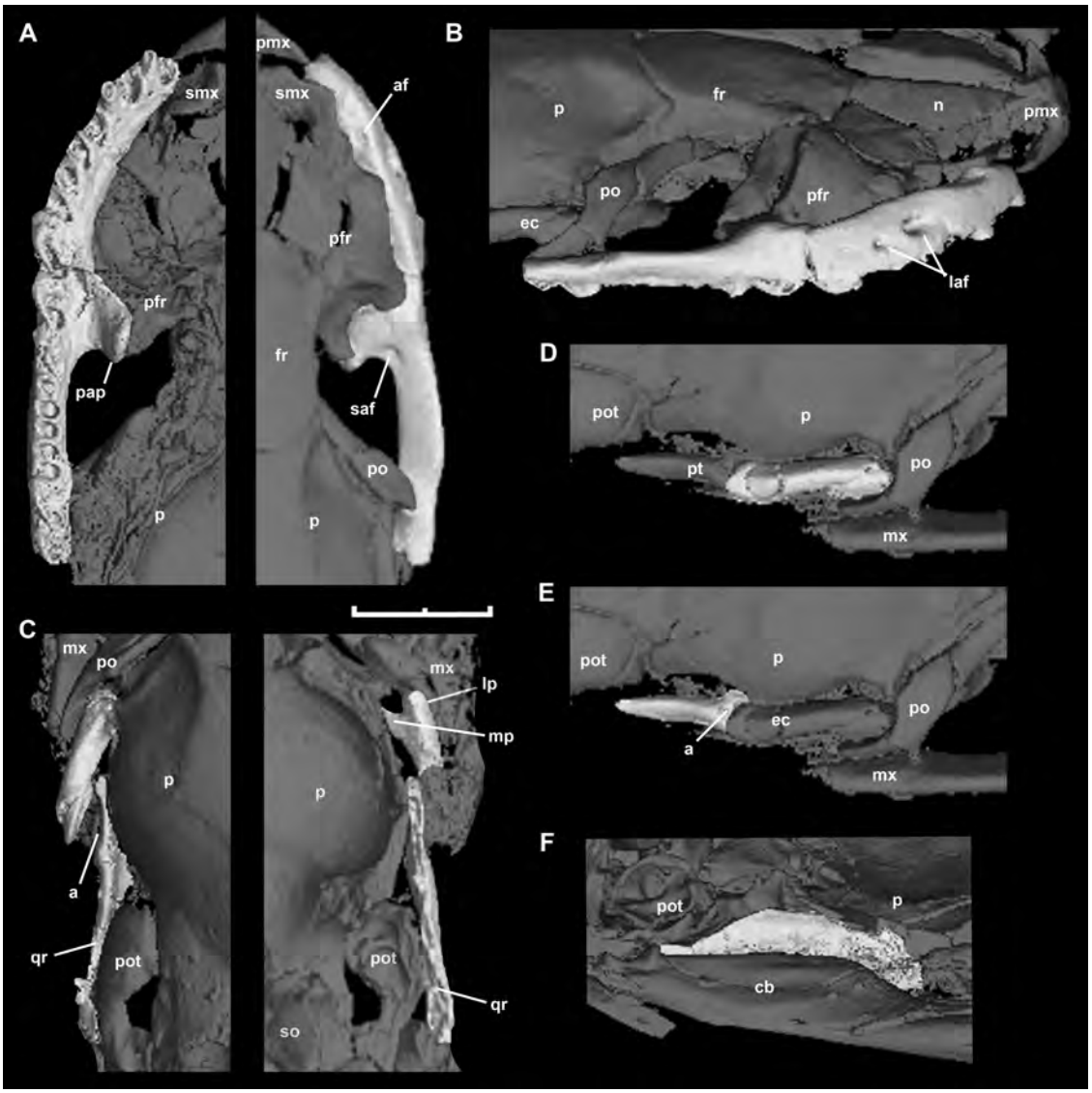

Figure 11. Three-dimensional reconstruction of the palatomaxillary bar components of the paratype specimen of *Messelophis ermannorum* (HLMD-Me 7915) based on HRXCT data. Scale bar equals 2 mm. Abbreviations: a, articular surface for the ectopterygoid; af, anterior medial foramen; cb, compound bone; fr, frontal; laf, labial foramen; lp, anterolateral prong; mp; anteromedial prong; mx, maxilla; n, nasal; p, parietal; pfr, prefrontal; pmx, premaxilla; po, postorbital; pot, prootic; pap, palatine process; qr, quadrate ramus; saf, foramen for the superior alveolar nerve; smx, septomaxilla; so, supraoccipital.

as in macrostomatans. As in most boids, both choanal and maxillary processes are located at the posterior end of the palatine, located on either side of the palatine–pterygoid joint. The choanal process comprises a narrow-based strip of bone, but the exact length of this process is not possible to ascertain. In the same way, the boundaries of the maxillary process are not defined in this specimen. Unfortunately, the poor preservation of this specimen precludes any interpretation about the nature of the palatine–pterygoid joint.

Frontal

Both frontals are present, but their lateral downgrowths are broken. In dorsal view, each frontal exhibits a rectangular shape and a slightly convex posterior border with the parietal. This bone lacks the supraorbital shelf that is consistently present in boines and that confers the square shape in dorsal view. In ventral view, it is possible to distinguish a well-developed medial frontal pillar, which is a typical alethinophidian trait (Rieppel, 2007).

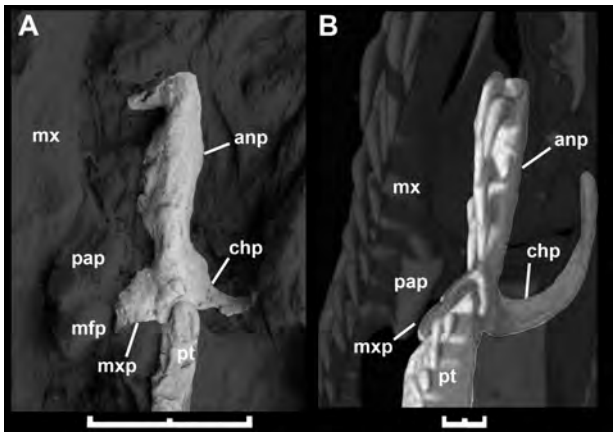

Figure 12. Palatine bone of *Messelophis ermannorum* (SMF ME 11426) coated with ammonium chloride (A), and three-dimensional reconstruction of the palatomaxillary bar components of the boid *Chilabothrus striatus* based on HRXCT data (B). Scale bars: 2 mm. Abbreviations: anp, anterior (dentigerous) process; chp, choanal process; mfp, medial foot process; mx, maxilla; mxp, maxillary process; pap, palatine process; pt, pterygoid.

Parietal

As was described by Schaal & Baszio (2004), the parietal of this species is broad anteriorly (Fig. 13C), a common condition in small-sized booids. As in *M. variatus* and other small booids, such as *Ungaliophis*, there are small supraorbital processes that embrace the posterior part of the frontals and give the parietal a concave anterior margin. The anterolateral corner bears a narrow shelf that extends from the supraorbital process to the postorbital process, and supported the dorsal end of the postorbital. A cup-shaped parietal table is well developed. Consequently, the sagittal crest is restricted to the posterior third of the bone. This crest continues posteriorly as a pointed posterior sagittal process, as in *M. variatus*, erycines, and boines, concealing the mid-sagittal region of the supraoccipital bone. The supratemporal process is present as a posteriorly directed lobe that covers part of the anterolateral corner of the supraoccipital. Laterally, this process exhibits a conspicuous longitudinal depression that received the anterior region of the supratemporal bone (Fig. 13C); this depression is absent in *M. variatus*. The mCT reconstruction reveals the endocranial view of the parietal of HLMD-Me 7915. As can also be inferred from the external view, the endocranial form of the parietal clearly shows a bulbous cavity for the telencephalon. Also, a strong medial parietal pillar, a typical feature present in all alethinophidian snakes, is well developed and delimits the space occupied by the telencephalic and mesencephalic regions of the brain.

Prootic

Little of the prootic bones is preserved: only the dorsal region that contacts the skull roof. Therefore, the extensive crushing of these preserved portions precludes any description of the most relevant features of this braincase bone. A depression that is a continuation of the respective structure on the parietal is present in the dorsal region of the right prootic. The combined depression received the anterior portion of the supratemporal bone.

Supraoccipital

Superficial examination and the CT reconstruction of HLMD-Me 7915 reveals the external and internal structure of the supraoccipital. It is extensively exposed in dorsal view, in contrast to boines and *Eryx*, where it is poorly exposed or not at all; however, as in these extant snakes the posterior process of the parietal covers the sagittal crest dorsally. Curving anteromedially and then posterolaterally from the distal end of the posterior process of this crest are the paired nuchal crests, which barely continue onto the otooccipitals. As in most macrostomatans (except tropidophiids and caenophidians) a pointed projection of the supraoccipital is interposed between the paired otooccipital atlantal processes. The internal view of the supraoccipital shows that the supraoccipital contributes to the dorsomedial part of the vestibular cavity, as in other snakes.

Otooccipital

Only the dorsal region of this bone is preserved in HLMD-Me 7915 (Fig. 14C). As a result of the displacement of the right supratemporal, the small paroccipital process can be seen. Amongst booids, relicts of the paroccipital process are present in pythonines, which display a relatively long spike-like structure, and in most boines and *Ungaliophis* (Fig. 14G). In this latter genus, as in *M. ermannorum*, the paroccipital process is represented by a small, acuminate projection of the posterolateral corner of the otooccipital. Both otooccipitals meet dorsally in a broad dorsomedial contact behind the supraoccipital (Fig. 14C), their atlantal crests forming the dorsal margin of the foramen magnum.

Quadrate

Both quadrates are preserved in HLMD-Me 7915 and SMF ME 11426. The quadrate of *M. ermannorum* has a broad cephalic condyle that lacks a suprastapedial process, and the shaft is relatively short (Fig. 15A). The stapedial contact, that is the stylohyal, lies at the posterior end of the cephalic condyle (Fig. 15B), as in small booids such as *Ungaliophis* (Fig. 15D, E) and *Exiliboa*. The mandibular condyle is broken medially; however, the preserved lateral portion suggests the condyle exhibited the typical saddle-shaped articular surface of most snakes. The quadrate is suspended from the pos-

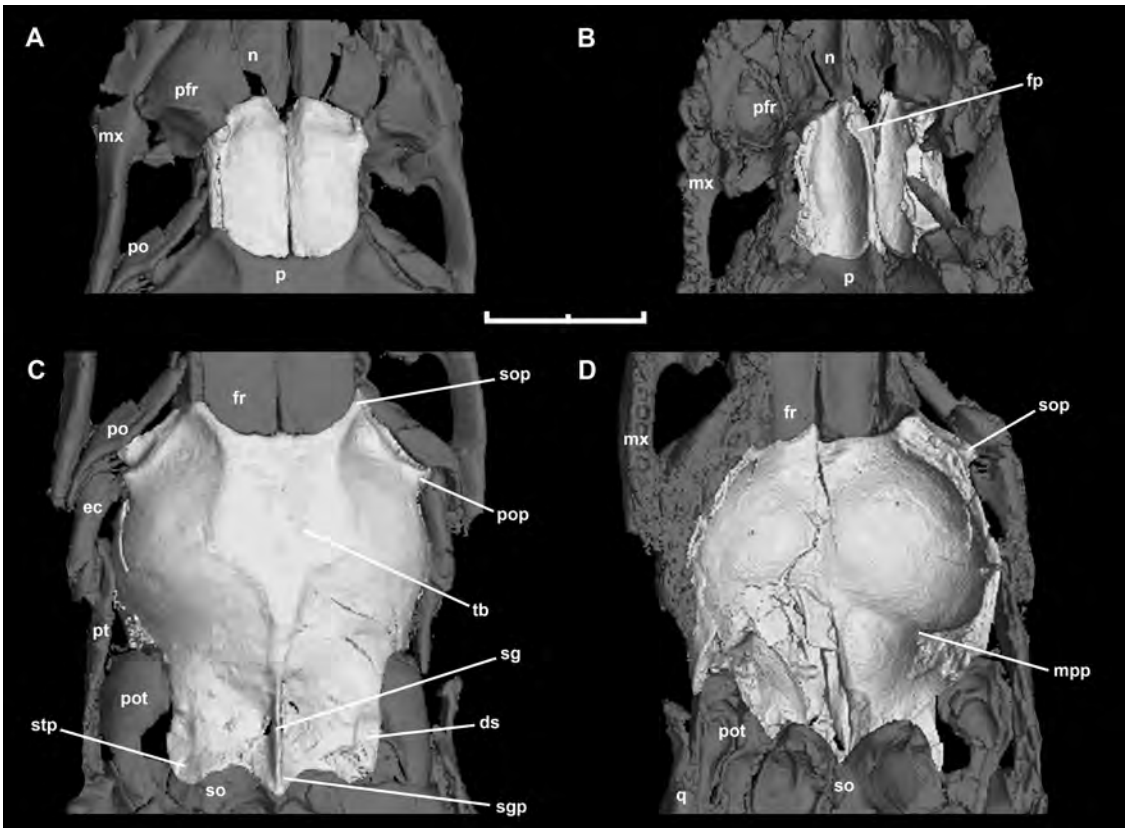

Figure 13. Three-dimensional reconstruction of the skull roof elements of the paratype specimen of *Messelophis ermannorum* (HLMD-Me 7915) based on HRXCT data. Scale bar: 3 mm. Abbreviations: ds, depression that receives the supratemporal bone; ec, ectopterygoid; fr, frontal; mpp, medial parietal pillar; mx, maxilla; fp, medial frontal pillar; n, nasal; p, parietal; pfr, prefrontal; po, postorbital; pot, prootic; pop, postorbital process; pt, pterygoid; sg, sagittal crest; sgp; sagittal process; so, supraoccipital; sop, supraorbital process; stp, supratemporal process; tb, parietal table.

terior portion of the supratemporal. Because the posterior end of the latter bone does not project as a free-ending process beyond the otooccipital (Fig. 15C), the mandibular condyle of the quadrate lies at the level of the occipital condyle.

Supratemporal

Left and right supratemporals are preserved in HLMD-Me 7915, although they are displaced from their anatomical position. The supratemporal of *M. ermannorum* is relatively short, with two different regions (Fig. 15C). The anterior portion is a tongue-like lappet that fits into the previously described depression on the supratemporal process of the parietal, the dorsal margin of the prootic, and the distal portion of the supraoccipital (Fig. 14A–C). The contour of this complex area of contact allows us to infer the position of the supratemporal in life, which was mostly applied above the braincase, and in particular the location of its anterior tip (Fig. 15C). This location shows that the supratemporal projected slightly beyond the rear margin of the otooccipital, a widespread condition among small-sized booids like *Ungaliophis* (Fig. 15F). The posterior free-ending portion exhibits a marked lip, obliquely oriented with respect to the supratemporal body, which received the quadrate cephalic condyle.

Lower jaw

The left lower jaw of HLMD-Me 7915 is almost completely preserved (Fig. 16). Schaal & Baszio (2004) mentioned only 13 teeth in the dentary of *M. ermannorum*, but the mCT reconstruction demonstrates that 23 tooth positions are present. Preserved teeth occupy several of these sockets, which are implanted as in alethinophidians (see Zaher & Rieppel, 1999). As in a number of macrostomatans, there is a distinct anteroposterior decrease in tooth size, although the difference between anterior and posterior teeth is not as marked as in some boids, like *Eryx* (Fig. 16F). The teeth exhibit a conical shape, and the tooth tips are recurved. The alveolar ramus of the trigeminal nerve emerges from a large mental foramen located at the posterior region of a shallow groove approximately positioned between the sixth and seventh teeth, whereas in

Figure 14. Three-dimensional reconstruction of braincase elements of the paratype specimen of *Messelophis ermannorum* (HLMD-Me 7915) based on HRXCT data in dorsal view (A, C) and endocranial view (B); dorsal view of braincase of the boine *Chilabothrus striatus* (D) and *Ungaliophis continentalis* (E), based on HRXCT data; F, three-dimensional cutaway view along the frontal axis of the braincase of *Ungaliophis continentalis*, based on HRXCT data. Scale bar: 2 mm. Abbreviations: at, atlantal crest; ds, depression that receives the supratemporal bone; nc, nuchal crest; ot, otooccipital; p, parietal; pa, paroccipital process; pot, prootic; q, quadrate; sg, sagittal crest of the supraoccipital; so, supraoccipital; st, supratemporal.

M. variatus the same foramen is at the fourth tooth position. The posterior dentigerous process is well developed, surpassing the limits of the posterior ventral process. Meckel's canal is deep and reaches the anterior tip of the bone. The left compound bone is well preserved. As in other alethinophidians, it bears an elongated mandibular fossa delimited by surangular and prearticular crests. As in *Eryx* (Fig. 16F), the long and straight surangular crest runs from the coronoid prominence anteriorly to the glenoid fossa; it is relatively weak in comparison with *M. variatus*. In medial view, the prearticular crest displays a convex dorsal edge. The surangular process of the compound bone has a particularly rounded anterior tip, in contrast with the anterior pointed process present in *M. variatus* and most snakes. The retroarticular process is short and robust. A relatively large coronoid bone is applied to the medial surface of the coronoid prominence and anterior part of the compound bone. Its anteroventral process is well developed and extends ventrally to meet the angular and splenial, although postmortem displacement separated it slightly from these postdentary bones. The splenial and angular bones are pierced by the anterior and posterior mylohyoid foramina, respectively. These bones meet in a straight vertical contact, thus forming the intramandibular joint, with articular facets on the splenial and dentary to accommodate processes of the coronoid and angular. At the joint, the splenial has a prominent anterodorsal spine that covers Meckel's groove and bounded the anterior inferior alveolar nerve.

Phylogenetic analysis

In order to test previous conclusions about the phylogenetic relationships of *M. variatus* and *M. ermannorum*, we performed morphology-based and combined (morphology + DNA) phylogenetic analyses. The 156-character morphological matrix of Scanferla *et al*. (2013) was modified slightly for this purpose. We changed several terminals to species level in order to diminish the number of polymorphic codings, and added several terminals that represent all recognized groups of macrostomatans (Boinae, Pythoninae, Erycinae, Ungaliophiinae, Tropidophiidae, and Bolyeriidae). Nine additional characters were obtained from the literature (Kluge, 1991, 1993a, b; Gauthier *et al*., 2012), and four new unpublished characters were defined from personal observations. The resulting matrix with 169 osteological characters was analysed alone and in com-

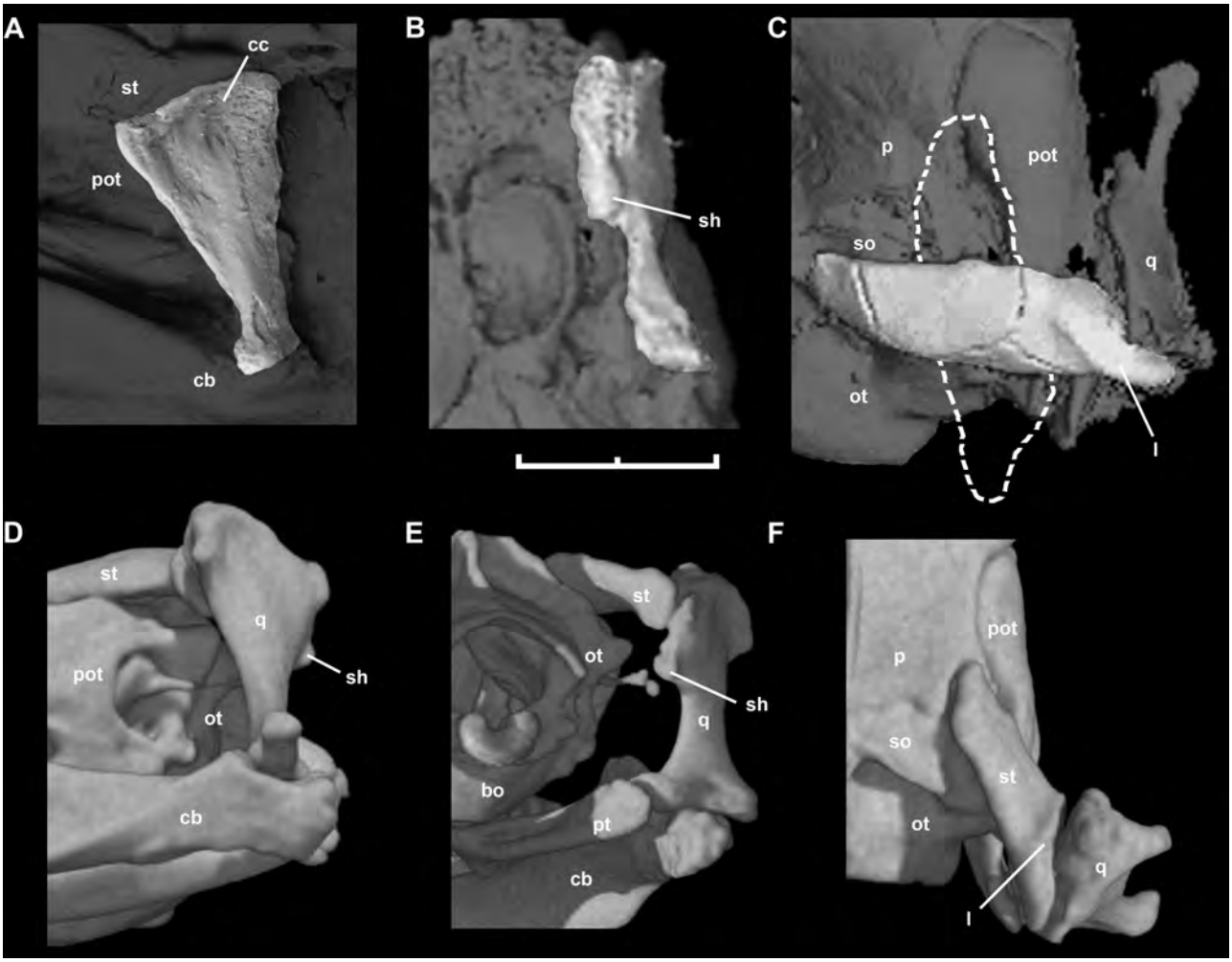

Figure 15. Three-dimensional reconstruction of quadrate and supratemporal of the paratype specimen of *Messelophis ermannorum* (HLMD-Me 7915), based on HRXCT data. Scale bar: 2 mm. Abbreviations: bo, basioccipital; cb, compound bone; cc, cephalic condyle; l, supratemporal lip that receives the quadrate; ot, otooccipital; p, parietal; pot, prootic; pt, pterygoid; q, quadrate; sh, stylohyal; so, supraoccipital; st, supratemporal.

bination with DNA sequences for four mitochondrial (*12S*, *16S*, cytochrome *b*, and *NADH4*) and four nuclear (*BDNF*, *Cmos*, *PNN*, and *NGFB*) genes, all taken from GenBank. The choice of these particular genes corresponds with their availability in GenBank for selected terminals in order to reduce the quantity of missing data. If multiple sequences were available in GenBank for a given taxon, we selected only one sequence and chose the most complete sequence for inclusion. We employed static homology via multiple alignment using default settings in Clustal X (Thompson *et al*., 1997). After alignment, each sequence was trimmed of its leading and lagging gaps using BIOEDIT (Hall, 1999). Thus, the resulting lengths of the DNA sequences in base pairs and gaps are: (317) *12S*, (354) *16S*, (519) cytochrome *b*, (522) *NADH4*, (658) *BDNF*, (295) *Cmos*, (507) *NGFB*, and (899) *PNN*. See Appendix S1 for further information.

Our morphological and combined matrices contain 37 taxa coded for 169 (morphological) and 4240 (169 morphological + 4071 molecular) characters (available at MorphoBank, http://www.morphobank.org, as project P1179). The trees were rooted using the anguimorph lizard *Varanus salvator* (Laurenti, 1768) as an outgroup, based on recently proposed anguimorph–snake relationships (Forstner, Davis & Arévalo, 1995; Lee, 2009; Wiens *et al*., 2010). The matrices were analysed in TNT (Goloboff, Farris & Nixon, 2008), with all characters treated as unordered and gaps coded as missing data. The general analytical method employed was maximum parsimony (Farris, 1983). The search strategy employed in TNT was 'Traditional

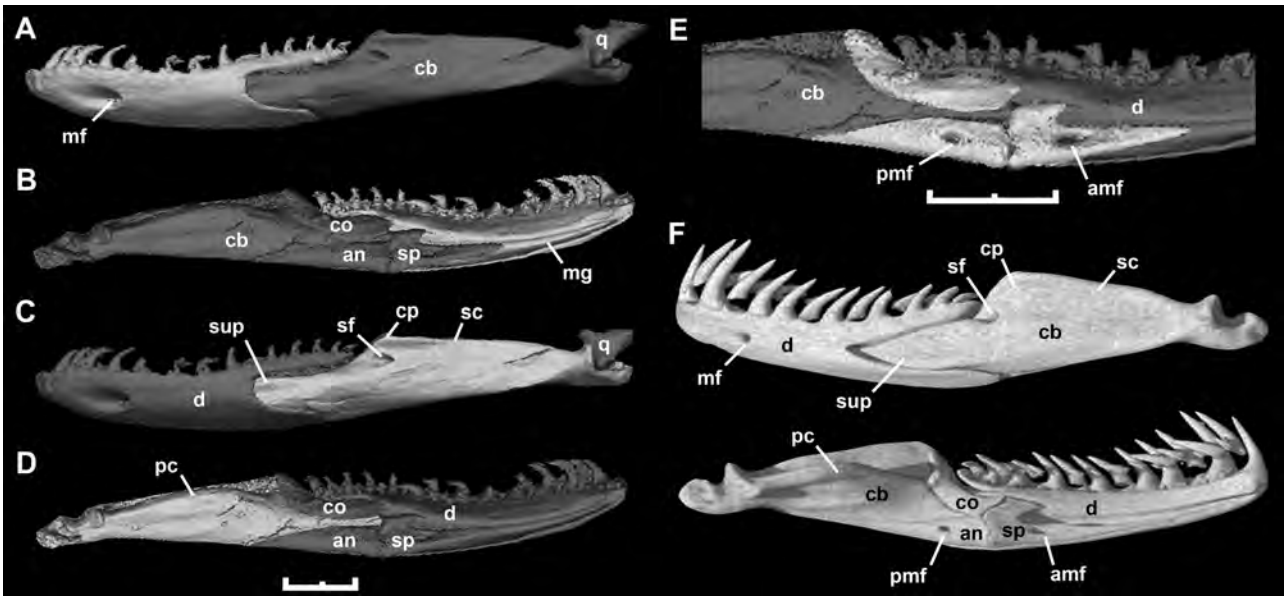

Figure 16. Three-dimensional reconstruction of the lower jaw of the paratype specimen of *Messelophis ermannorum* (HLMD-Me 7915), based on HRXCT data. Lateral (A) and medial (B) view of left dentary; lateral (C) and medial (D) view of left compound bone; medial view of left coronoid, angular, and splenial bones (E). F, three-dimensional reconstruction based on HRXCT data of lateral and medial view of the lower jaw of *Eryx colubrinus*. Scale bars: 2 mm. Abbreviations: amf, anterior mylohyoid foramen; an, angular; cb, compound bone; co, coronoid; cp, coronoid prominence; d, dentary; mf, mental foramen; mg, Meckelian groove; pc, prearticular crest; pmf, posterior mylohyoid foramen; q, quadrate; sc, surangular crest; sf, anterior surangular foramen; sp, splenial; sup, surangular process.

search' (using tree bisection and reconnection, TBR) with 1000 replications, with the objective of encountering all possible tree islands. Two alternative support measures (Bremer support and bootstrap resampling) were obtained with TNT to evaluate the robustness of the nodes of the most parsimonious trees. Bootstrap values were calculated with 1000 pseudoreplicates.

Despite the incompleteness of *Messelophis* species and of several other fossils added to the analysis, the obtained trees exhibit rather good resolution and strong support values for several nodes (Fig. 17). The analysis including all taxa and morphological characters yielded eight most-parsimonious trees, each with 456 steps (consistency index, CI 0.46; retention index, RI 0.75), whereas the analysis of the combined data set (morphological plus DNA) yielded one most-parsimonious tree with 6332 steps (CI 0.48; RI 0.41). Despite some topological differences with respect to fossil Indoaustralian 'madtsoiids' and marine simoliophiids, both consensus trees show a similar internal arrangement for Macrostomata. The only remarkable difference between them is the placement of pythonine snakes, which are nested with the rest of booid clades in the morphological analysis, whereas in the combined analysis they form, together with *Xenopeltis* and *Loxocemus*, an exclusive clade located at the base of Macrostomata. Despite the differences mentioned above, we recover *M. variatus* and *M. ermannorum* nested in a clade formed by ungaliophiines, erycines, and boines, i.e. the family Boidae *sensu* Vidal, Delmas & Hedges (2007). This clade is supported by 30 molecular and four morphological synapomorphies, three of them unambiguous and unreversed (see Appendix S1). Nevertheless, only two of these synapomorphies could be scored in *Messelophis* specimens: the presence of a long finger-like medial foot process in the prefrontal (character 30) and the posterior position at the level of the palatine–pterygoid joint of the maxillary process of the palatine (character 76).

DISCUSSION

Phylogenetic relationships of minute Messel boas

The results of the phylogenetic analyses performed here demonstrate the booid relationships of the minute Messel boas, a signal that is recovered with both morphological and combined evidence. One feature, the presence of a well-developed finger-like medial foot process in the prefrontal bone, represents an unambiguous synapomorphy of this booid clade that is clearly seen in both *M. variatus* and *M. ermannorum*. In the origi-

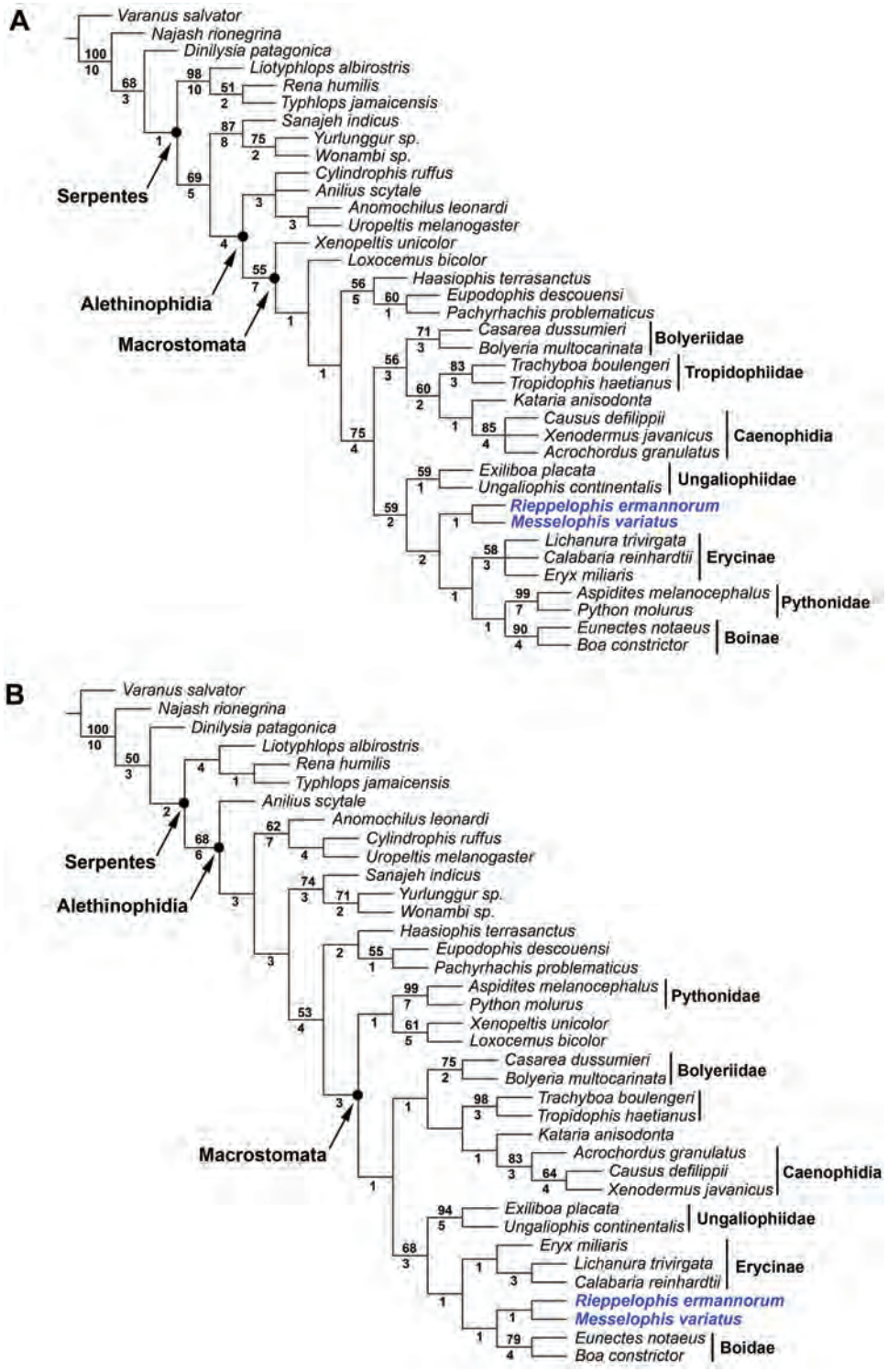

Figure 17. Maximum-parsimony cladograms of snake relationships depicting the placement of Messel minute boas: A, strict consensus of the eight trees obtained (tree length, L = 456) based on osteological characters; B, most parsimonious tree (L = 6332) based on the combined analysis of morphological, mitochondrial, and nuclear data partitions. Bootstrap (above) and Bremer support (below) values for each node are indicated. Note the position of *Messelophis variatus* and *Messelophis ermannorum* (in blue) nested into the boid clade in both cladograms.

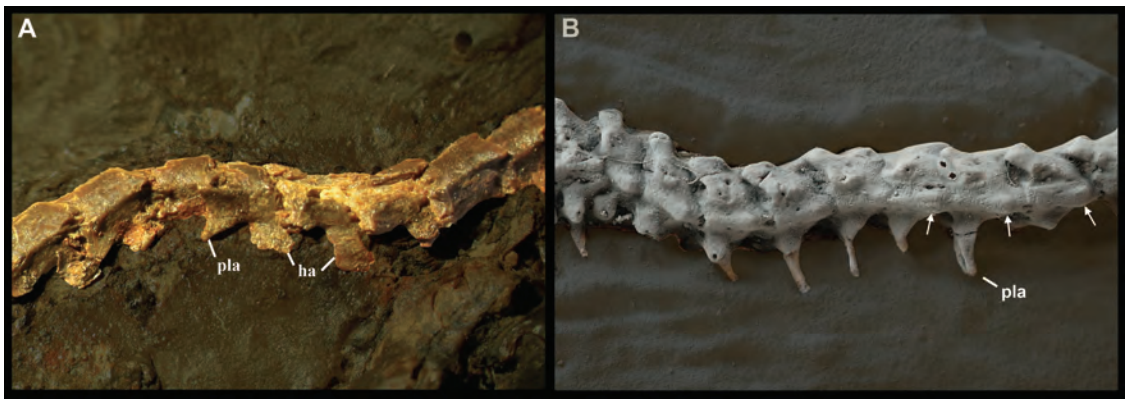

Figure 18. Caudal anatomy of Messel minute boas: A, lateral view of a string of eight postcloacal (probably medial) vertebrae of the holotype specimen of *Messelophis variatus* (SMF ME 1828 a+b); B, ventrolateral view of postcloacal vertebrae of the paratype specimen of *Messelophis ermannorum* (HLMD-Me 7915), coated with ammonium chloride. Arrows indicate the position of ventral protuberances. Not to scale. Abbreviations: ha, haemapophysis, pla, pleuroapophysis.

nal description of *Messelophis* species, Baszio (2004) and Schaal & Baszio (2004) mainly used the vertebral morphology to infer the phylogenetic allocation of these fossil snakes. They proposed that some vertebral traits, in particular the position and development of the neural spine, resemble the morphology present in the extant genera *Ungaliophis* and *Exiliboa*. It is important to note that these authors (following palaeontological tradition) considered ungaliophiine snakes to be closely related to *Tropidophis* and *Trachyboa*, with all four genera forming the subfamily Tropidopheinae; however, this phylogenetic arrangement has been refuted by our analyses and nearly all recent morphological (Zaher, 1994; Tchernov *et al*., 2000; Lee & Scanlon, 2002; Wilson *et al*., 2010; Gauthier *et al*., 2012; Scanferla *et al*., 2013), molecular (Wilcox *et al*., 2002; Noonan & Chippindale, 2006; Wiens *et al*., 2008, 2012; Pyron, Burbrink & Wiens, 2013), and combined analyses (Lee *et al*., 2007; Scanlon & Lee, 2011; Reeder *et al*., 2015) of snake relationships.

Despite the generally high resolution of our phylogenetic analyses, the poor support for internal nodes within Boidae precludes more precise phylogenetic inferences about the relationships of minute Messel boas with respect to boines, erycines, and ungaliophiines. This fact clearly indicates the need for further work on this part of the ophidian tree. Regrettably, some important pieces of evidence, such as the basicranium, are not preserved in known specimens of either species of *Messelophis*. Recently, Smith (2013) emphasized the relevance of the anatomy of postcloacal vertebrae to establish the relationships of fossil small boas. *Ungaliophis* and *Exiliboa* lack the typical paired haemapophyses throughout the postcloacal region, which are replaced by a haemal keel (Smith, 2013: fig. 7; see also Szyndlar & Rage, 2003). Although the caudal region of *Messelophis* species was not previously described, we observed the presence of well-developed laminar and paired haemapophyses in a string of postcloacal vertebrae of the holotype specimen of *M. variatus* (SMF ME 1828 a+b; Fig. 18A). These structures are very similar to those of numerous macrostomatans, where haemapophyses originate from the posterior region of the ventral part of the vertebral centrum and point ventrally. Surprisingly, the postcloacal vertebrae of *M. ermannorum*, well preserved in the paratype specimen HLMD-Me 7915 (Fig. 18B), display a contrasting morphology, where paired haemapophyses are absent as in ungaliophiines, and instead there are two indistinct protuberances ventral to the condyle, similar to the Oligocene small booid-like macrostomatan *Rottophis atavus* von Meyer, 1855 (Szyndlar & Böhme, 1996). Additionally, the distal postcloacal vertebrae of *M. variatus* and *M. ermannorum* completely lack the derived accessory structures present in *Eryx*, and in the North American erycines *Charina* and *Lichanura*.

Beyond the phylogenetic placement of minute Messel boas discussed above, our cladistic hypothesis has two topological aspects that merit further discussion. In contrast to traditional hypotheses based on morphology, molecular (e.g. Vidal & Hedges, 2002; Wilcox *et al*., 2002; Vidal *et al*., 2007; Wiens *et al*., 2012; Pyron *et al*., 2013) and combined analyses of extensive morphological and molecular data sets (Scanlon & Lee, 2011; Reeder *et al*., 2015) persistently retrieve a paraphyletic Macrostomata as a result of the placement of tropidophiids with the basal alethinophidian *Anilius* in a clade denominated 'Amerophidia' (Vidal *et al*., 2007) at the base of Alethinophidia. The other recurrent disparate result of molecular and combined analyses is the placement of pythons together with the basal macrostomatans *Xenopeltis* and *Loxocemus* in a clade at the base of

Macrostomata. Surprisingly, our combined analysis found a monophyletic Macrostomata, where tropidophiids constitute the sister group of a clade composed by the Palaeocene-derived macrostomatan *Kataria* and caenophidians (represented in our analyses by *Acrochordus*, *Xenodermus*, and the viperid *Causus*). This phylogenetic arrangement is identical to the traditional hypothesis obtained in all morphological analyses published to date (e.g. Cundall, Wallach & Rossman, 1993; Tchernov *et al*., 2000; Lee & Scanlon, 2002; Wilson *et al*., 2010; Gauthier *et al*., 2012; Zaher & Scanferla, 2012; Scanferla *et al*., 2013). Nevertheless, in our analysis pythons form a clade with *Xenopeltis* and *Loxocemus* at the base of Macrostomata, in congruence with molecular and combined analyses. Evidently, the arrival of molecular phylogenetics has shaken the snake tree and demands revision to our thinking about some issues of snake systematics. Hence, the recurrence of phylogenetic signals that indicate the repeated appearance or loss of osteological requisites to macrostomy (see Cundall & Irish, 2008) suggests the necessity to test the hypothesis of homology about these crucial morphological traits. Our study of *Messelophis* species highlight this need, because these minute snakes lack the typical elongation of the gnathic complex (i.e. palatomaxillary arch, supratemporal, quadrate, and mandible) present in adults of most extant macrostomatans that show macrostomy.

Fossil calibration point

The completeness and phylogenetic information provided by the several specimens of *Messelophis* result in an excellent calibration point for the clade Booidea (Boinae, Erycinae, *Exiliboa*, and *Ungaliophis*). We follow the recommendations made by Parham *et al*. (2012) to establish an accurate fossil calibration point for this clade: (1) as reference specimens, we propose the holotype of *M. variatus* (SMF ME 1828 a+b) and the paratype specimen of *M. ermannorum* (HLMD-Me 7915); (2) our combined analysis is an explicit phylogenetic analysis of the taxa; (3) our combined analysis gives a statement about morphological and molecular reconciliation; (4) proposed specimens were found in the World Natural Heritage Messel Pit fossil site near Darmstadt (Germany), in levels of the Middle Eocene (Early Lutetian, MP11) Middle Messel Formation; and (5) a minimum age of 47.4 Mya for the Middle Messel Formation, based on astronomical tuning and revised $^{40}Ar/^{39}Ar$ ages (youngest age model; Lenz *et al*., 2015).

Mode of life of the minute Messel boas

On the basis of individual vertebral features – reduced neural spine, and measurements of an 'anti-torsion-complex' of the vertebral column (features never described by the author) – Baszio (2004) proposed that *M. variatus* and *M. ermannorum* were largely terrestrial species that dwelled in leaf litter. In particular, he excluded a primarily fossorial mode of life by noting that *M. variatus* has a much higher number of vertebrae (~ 300) than three reputedly burrowing taxa (*Exiliboa*, *Lichanura*, and *Eryx*). He concluded by suggesting that this snake was a 'terrestrial tropidopheine with a weak tendency to burrow' (Baszio, 2004: 64). Similar statements about a fossorial or burrowing mode of life in extinct snakes are commonly found in the literature, sometimes qualified as 'semi-fossorial' or 'partially burrowing' (e.g. Hecht, 1982; Apesteguía & Zaher, 2006; Longrich *et al*., 2012). This inference is typically made from the vertebral morphology, especially with respect to the development of the neural spine.

Many extant snakes, particularly the small species, hide below different kinds of natural shelters (leaf litter, bark, rocks), whereas others also occupy complex tunnels of their own construction. Although the behaviour of species in the first group may not be associated with clear osteological traits, the active burrowers of the second group – blindsnakes (Scolecophidia), basal alethinophidians like uropeltids, and some macrostomatans – display common anatomical traits that can be observed in the skeleton, which are in turn useful for accurately inferring a burrowing mode of life in extinct snakes. Active head-first burrowers generally exhibit a small cylindrical body with a smooth integument, shortening of the tail, and reduced eyes (Gans, 1974). The skull structure of these burrowing snakes bears an extensive dorsoventral contact of the nasal medial flanges with the medial frontal flanges, reduction of rhinokinesis produced by overlapping joints between skull roof bones and the rest of the skull, flattening and expansion of the premaxilla transverse processess, shortening of the jaw suspensorium and palatomaxillary arch, narrowing of the braincase, and reduction of the neural spine of mid-posterior precloacal vertebrae (Norris & Kavanau, 1966; Hoffstetter & Gasc, 1969; Gans, 1974; Rieppel, 1978; Savitzky, 1983; Rieppel, 2007). These characters are correlated with an overall reduction of friction with the substrate and a strengthening of the rostral region to resist the mechanical stress produced during the penetration of the substrate (Gans, 1974; Wake, 1993).

The morphology of *M. variatus* and *M. ermannorum* described herein demonstrates that these fossil snakes possess a generalized macrostomatan cranial pattern, and thus lack nearly all of the aforementioned traits present in the skeleton of extant burrowing snakes. Even though the small or minute size of the neural spines of these fossil snakes could be invoked to infer a burrowing behaviour, extant surface-dwellers such as *Ungaliophis* are similar in size to the minute Messel

boas. Thus, based on the above considerations we agree that there is no evidentiary basis for assuming burrowing habits in the minute Messel boas. Snakes with a generalized skull morphology by definition lack adaptations to a burrowing mode of life, even if they indeed had burrowing habits. Thus, inferences about burrowing habits in fossil snakes should be formulated by taking into account general shape traits that can be ascertained from the skeleton (e.g. body length, tail length, and orbit size), together with the anatomy of rostral region.

Relationships with other European Palaeogene small 'booid' snakes

Palaeogene strata from Europe have yielded one of the most comprehensive records of snakes from the Northern Hemisphere; however, the European record is still patchy with respect to cranial and postcranial associated specimens. In fact, the Messel taxa are the most complete fossil snakes ever described from this continent. Of the European Palaeogene snakes known or thought to preserve cranial and postcranial elements, the minute Messel boas most closely resembles *Platyspondylia*. This genus was erected by Rage (1974) for the reception of a small booid-like snake represented by some cranial bones and vertebrae found in the Late Oligocene of Phosphorites du Quercy, France. Based on vertebrae, this genus is present in other localities of Europe from the late Eocene to the late Oligocene (Szyndlar & Rage, 2003). Previous authors considered that this snake shares several traits with ungaliophiine snakes (McDowell, 1987; Szyndlar & Rage, 2003), such as the morphology of the vertebrae, compound bone, etc.

In the course of our revision of *Messelophis* species, we observed that preserved cranial bones attributed to *Platyspondylia* exhibit similarities with those of the minute Messel boas, especially *M. ermannorum*. The compound bone of these snakes (Fig. 19A–D) exhibits a rectilinear surangular crest that runs from a low coronoid prominence to the glenoid fossa. The prearticular crest also resembles the morphology in *M. ermannorum*, where this convex crest is slightly lower than the surangular crest. The quadrate bone is very similar (Fig. 19E, F), with a wide and flat cephalic condyle, and the fused stylohyal is located at the posterior end of the cephalic condyle. No European fossil snake except *Platyspondylia* displays the very small size of the minute Messel boas, and the morphology of cranial bones and vertebrae suggest that these snakes could represent a European lineage of Palaeogene small boid snakes; however, this assertion should be taken with caution until more, and closely associated, materials of *Platyspondylia* are found.

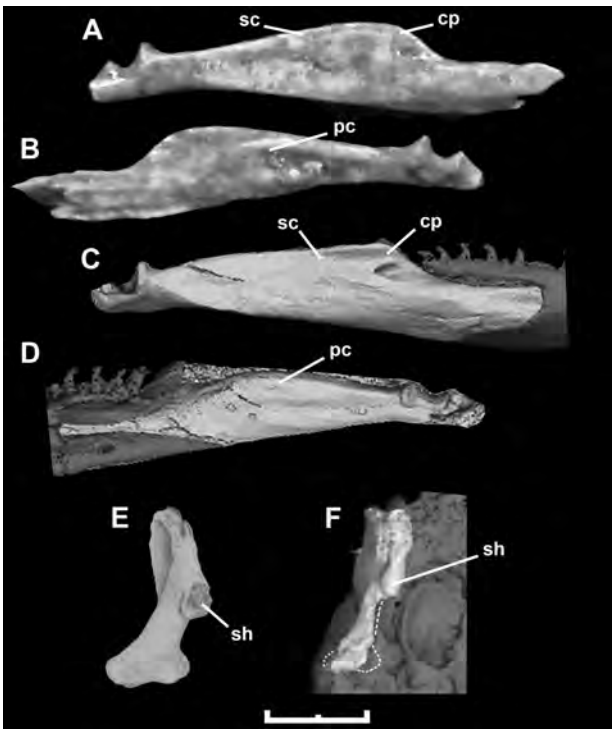

Figure 19. Comparisons between cranial elements of *Platyspondylia lepta* and *Messelophis ermannorum*. Lateral (A) and medial (B) views of right compound bone of *P. lepta* (MNHN PFR 6357); lateral (C) and medial (D) views of three-dimensional reconstruction of the lower jaw of the paratype specimen of *M. ermannorum* (HLMD-Me 7915), based on HRXCT data; posterior view of left quadrate of *P. lepta* (MNHN PDS 3118) (E) and *M. ermannorum* (F). Scale bar: 2 mm. Abbreviations: cp, coronoid prominence, pc, prearticular crest, sc, surangular crest, sh, stylohyal.

Reappraisal of the taxonomy of minute Messel boas

Although several specimens of both *Messelophis* species have been recovered with skulls in different states of preservation, the original diagnoses of both species were made based almost exclusively on vertebral characters. Schaal & Baszio (2004) stated in the differential diagnosis of *M. ermannorum* that this species differs from *M. variatus* in the structure of the neural spine of precloacal vertebrae (very short and point-like in all vertebrae of *M. variatus*) and the presence of a haemal keel (absent in *M. variatus*); Baszio (2004) also noted differences in the premaxilla (presence of teeth and general proportions). It is important to emphasize the difference in vertebral count between these species. Baszio (2004: table 3) reported that specimens of *M. variatus* bear 298–300 precloacal vertebrae and 74–80 cloacal/postcloacal vertebrae, versus 183 precloacal vertebrae and 36 cloacal/postcloacal

vertebrae in *M. ermannorum*. Such a difference in the number of vertebrae greatly surpasses the differences observed between extant congeneric species (Alexander & Gans, 1966: table 2). In the course of our revision of these fossil snakes we discovered numerous additional anatomical disparities between these species. In the postcranial skeleton, paired haemapophyses are present on postcloacal vertebrae of *M. variatus*, but (largely) absent in *M. ermannorum*. Additionally, there are several morphological disparities in the skull of these fossil snakes. Notably, *M. variatus* has a toothed premaxilla, but *M. ermannorum* lacks teeth in this rostral bone (Baszio, 2004). Baszio (2004) described the presence of one labial foramen in the maxilla of *M. variatus*, but our observations show that two are present in the paratype of *M. ermannorum*. The position of the mental foramen in the dentary also differs between these species. In *M. variatus*, the mental foramen is located at the fifth tooth position, whereas in *M. ermannorum* this foramen is at the seventh tooth position. Finally, another cranial difference is the curved ectopterygoid shaft in *M. variatus*, in contrast to the straight shaft in *M. ermannorum*. This cranial and postcranial disparity exceeds the morphological variation observed between congeneric species of extant snakes. The paucity of morphological differences in the skull anatomy of congeneric species of booid snakes is strikingly shown by Frazzetta's (1966) exhaustive comparisons of species of *Python*. He compared *Python molurus* (Linnaeus, 1758) and *Python sebae* (Gmelin, 1788), and found very few differences between them. In fact he described only two cranial features (the structure of the anterior portion of the ectopterygoid and one more tooth in the maxilla) that differ between these two species of pythons. In view of the contrasting morphological traits found in the cranial and postcranial skeleton of *M. variatus* and *M. ermannorum*,m and the weak evidence for their sister-group status (see above), we consider that the last species should be allocated to a different genus.

SYSTEMATIC PALAEONTOLOGY

SUBORDER SERPENTES LINNAEUS, 1758

INFRAORDER ALETHINOPHIDIA NOPCSA, 1923

MACROSTOMATA MÜLLER, 1831

FAMILY BOIDAE GRAY, 1825 *SENSU* VIDAL *ET AL.* (2007)

GENUS ***RIEPPELOPHIS* GEN. NOV.**

Etymology

In honour of Olivier Rieppel, who contributed extensively to our understanding of the evolution of snakes.

RIEPPELOPHIS ERMANNORUM (SCHAAL & BASZIO, 2004) **COMB. NOV.**

Holotype

SMF ME 1812, five trunk vertebrae.

Locality and horizon

Middle Messel Formation, Messel Pit near Darmstadt (Germany), middle Eocene (MP 11).

Diagnosis

A very small booid snake that can be distinguished from all other members of Serpentes by the following combination of characters: edentulous premaxilla with ascending process; nasal articulates with the medial frontal pillar; lacrimal duct opens ventrally; large finger-like medial foot process; postorbital applied to parietal and frontal; parietal with parietal table and a pointed posterior process in sagittal crest; maxilla with two maxillary foramina, and 22 tooth positions and teeth diminishing in size posteriorly; ectopterygoid with forked maxillary process; contact with the pterygoid via a concave surface in the lateral surface of the pterygoid; parietal table present; supraorbital process of parietal well developed; supratemporal short with a conspicuous lip in its contact region with the quadrate; ~ 183 precloacal and ~ 36 cloacal–postcloacal vertebrae; neural spine of precloacal vertebrae robust, occupying almost half the length of the neural arch; paracotylar foramina absent; prezygapophyseal process very weakly developed; haemal keel well developed; and paired haemapophyses in postcloacal vertebrae absent and replaced by barely defined paired protuberances located below of the condyle.

GENUS *MESSELOPHIS* BASZIO, 2004

MESSELOPHIS VARIATUS BASZIO, 2004

Holotype

SMF ME 1828 a+b, an articulated, almost complete skeleton, and SMF ME 1828 c, four isolated vertebrae extracted from the same specimen.

Locality and horizon

Middle Messel Formation, Messel Pit near Darmstadt (Germany), middle Eocene (MP 11).

Emended diagnosis

A minute booid snake that can be distinguished from all other members of Serpentes by the following combination of characters: dentate premaxilla with ascending process; lacrimal duct opens ventrally; large finger-like medial foot process; postorbital is applied to parietal and frontal; parietal with parietal table and a pointed posterior process in sagittal crest; maxilla with one large maxillary foramen, and teeth dimin-

ishing in size posteriorly; ectopterygoid with forked maxillary process; parietal table present; supraorbital process of parietal well developed; supratemporal short, with a conspicuous lip in its contact region with the quadrate; anterior dorsal and ventral processes of prootic weakly developed (i.e. anterior trigeminal foramen anteriorly delimited by parietal); laterosphenoid present; ~ 300 precloacal and 68–80 cloacal–postcloacal vertebrae; neural spine of precloacal vertebrae pointlike, shifted to the posteriormost part of the neural arch; prezygapophyseal process weakly developed; paracotylar foramina absent; haemal keel absent throughout the vertebral column; and paired laminar haemapophyses in postcloacal vertebrae present.

ACKNOWLEDGEMENTS

Michael Ackermann and Bruno Behr prepared the SMF specimens. We thank Julián Faivovich (MACN), Ivan Ineich and Jean-Claude Rage (MNHN), Darrell Frost, Mark Norell, and Carl Mehling (AMNH), and Jorge Williams (MLP) for access to the skeletal collections and loan of specimens. Jean-Claude Rage provided us with photographs and information about Palaeogene fossil snakes. Anika Vogel (SMF) most kindly took several useful photographs of Messel specimens. We are also grateful to Javier Ochoa for the skillful drawings. Anonymous reviewers gave thorough and constructive criticism. The phylogenetic analysis was performed with TNT, software that is freely available through the Willi Hennig Society.

REFERENCES

Alexander AA, Gans C. 1966. The pattern of dermal vertebral correlation in snakes and amphisbaenians. *Zoologische Mededelingen* **41:** 171–190.

Apesteguía S, Zaher H. 2006. A Cretaceous terrestrial snake with robust hindlimbs and a sacrum. *Nature* **440:** 1037–1040.

Baszio S. 2004. *Messelophis variatus* n. gen. nov. sp. from the Eocene of Messel: a tropidopheine snake with affinities to Erycinae (Boidae). *Courier Forschungsinstitut Senckenberg* **252:** 47–66.

Cundall D, Wallach W, Rossman DA. 1993. The systematic relationships of the snake genus *Anomochilus*. *Zoological Journal of the Linnean Society* **109:** 275–299.

Farris JS. 1983. The logical basis of phylogenetic analysis. In: Platnick NI, Funk VA, eds. *Advances in cladistics, Vol. 2*. New York: Columbia University Press, 7–36.

Forstner MR, Davis SK, Arévalo E. 1995. Support for the hypothesis of anguimorph ancestry for the Suborder Serpentes from phylogenetic analysis of mitochondrial DNA sequences. *Molecular Phylogenetics and Evolution* **4:** 93–102.

Frazzetta TH. 1966. Studies on the morphology and function of the skull in the Boidae (Serpentes). Part II. Morphology and function of the jaw apparatus in *Python sebae* and *Python molurus*. *Journal of Morphology* **118:** 217–296.

Gans C. 1974. *Biomechanics: an approach to vertebrate biology*. Philadelphia: J B Lippincott Co.

Gauthier JA, Kearney M, Maisano JA, Rieppel O, Behlke ADB. 2012. Assembling the Squamate tree of life: perspectives from the phenotype and the fossil record. *Bulletin Peabody Museum of Natural History* **53:** 1–308.

Goloboff PA, Farris JS, Nixon KC. 2008. TNT, a free program for phylogenetic analysis. *Cladistics: The International Journal of the Willi Hennig Society* **24:** 1–13.

Grein M, Utescher T, Wilde V, Roth-Nebelsick A. 2011. Reconstruction of the middle Eocene climate of Messel using palaeobotanical data. *Neues Jahrbuch für Geologie und Paläontologie, Abhandlungen* **260:** 305–318.

Hall TA. 1999. Bioedit: a user-friendly biological sequence alignment editor and analysis program for Windows 95/98/NT. *Nucleic Acids Symposium Series* **41:** 95–98.

Hecht MK. 1982. The vertebral morphology of the cretaceous snake *Dinilysia patagonica* Woodward. *Neues Jarbuch der Geologie und Paläontologie* **1982:** 523–532.

Hoffstetter R, Gasc JP. 1969. Vertebrae and ribs of modern reptiles. In: Gans C, Bellairs D'A, Parsons T, eds. *Biology of the reptilia 1*. New York: Academic Press, 201–310.

Kluge AG. 1991. Boine snake phylogeny and research cycles. *Miscellaneous Publications of the Museum of Zoology, Michigan University* **178:** 1–58.

Kluge AG. 1993a. *Calabaria* and the phylogeny of erycine snakes. *Zoological Journal of the Linnean Society* **107:** 293–351.

Kluge AG. 1993b. *Aspidites* and the phylogeny of pythonine snakes. *Records of the Australian Museum Supplement* **19:** 1–77.

Lee MSY. 2009. Hidden support from unpromising data sets strongly unites snakes with anguimorph 'lizards'. *Journal of Evolutionary Biology* **22:** 1308–1316.

Lee MSY, Scanlon JD. 2002. Snake phylogeny based on osteology, soft anatomy and ecology. *Biological Review* **77:** 333–401.

Lee MSY, Hugall AF, Lawson R, Scanlon JD. 2007. Phylogeny of snakes (Serpentes): combining morphological and molecular data in likelihood, Bayesian and parsimony analyses. *Systematics and Biodiversity* **5:** 371–389.

Lenz OK, Wilde V, Riegel W. 2011. Short-term fluctuations in vegetation and phytoplankton during the middle Eocene greenhouse climate: a 640-kyr record from the Messel oil shale (Germany). *International Journal of Earth Sciences* **100:** 1851–1874.

Lenz OK, Wilde V, Mertz DF, Riegel W. 2015. New palynology-based astronomical and revised 40Ar/39Ar ages for the Eocene maar lake of Messel (Germany). *International Journal of Earth Sciences* **104:** 873–889.

McDowell SB. 1987. Systematics. In: Seigel RA, Collins JT, Novak SS, eds. *Snakes: ecology and evolutionary biology*. New York: Macmillan, 3–50.

McNamara ME, Briggs DEG, Orr PJ, Wedmann S, Noh H, Cao H. 2011. Fossilized biophotonic nanostructures reveal the original colors of 47-million-year-old moths. *PLoS Biology* **9:** 1–8.

Morlo M, Schaal S, Mayr G, Seiffert C. 2004. An annotated taxonomic list of the Middle Eocene (MP 11) Vertebrata of Messel. *Courier Forschungsinstitut Senckenberg* **252:** 95–108.

Noonan BP, Chippindale PT. 2006. Dispersal and vicariance: the complex biogeographic history of boid snakes. *Molecular Phylogenetics and Evolution* **40:** 347–358.

Norris KS, Kavanau JL. 1966. The burrowing of the western shovel-nosed snake, *Chionactis occipitalis* Hallowell, and the understand environment. *Copeia* **1966:** 650–664.

Olori JC, Bell CJ. 2012. Comparative skull morphology of uropeltid snakes (Alethinophidia: Uropeltidae) with special reference to disarticulated elements and variation. *PLoS ONE* **7:** e32450. doi: 10.1371/journal.pone.0032450

Parham JF, Donoghue PCJ, Bell CJ, Calway TD, Head JJ, Holroyd PA, Inoue JG, Irmis RB, Joyce WG, Ksepka DT, Patane JSL, Smith ND, Tarver JE, Tuinen M, Yang Z, Angielczyk KD, Greenwood J, Hipsley CA, Jacobs L, Makovicky PJ, Mueller J, Smith KT, Theodor JM, Warnock RCM, Benton MJ. 2012. Best practices for justifying fossil calibrations. *Systematic Biology* **61:** 346–359.

Pyron RA, Burbrink FT, Wiens JJ. 2013. A phylogeny and revised classification of Squamata, including 4161 species of lizards and snakes. *BMC Evolutionary Biology* **13:** 1–53.

Rage J-C. 1974. Les serpents des Phosphorites du Quercy. *Palaeovertebrata* **6:** 274–303.

Rage J-C, Szyndlar Z. 2005. Latest Oligocene–Early Miocene in Europe: dark period for booid snakes. *Comptes Rendus Palevol* **4:** 428–435.

Reeder TW, Townsend TM, Mulcahy DG, Noonan BP, Wood PL Jr, Sites JW, Wiens JJ. 2015. Integrated analyses resolve conflicts over squamate reptile phylogeny and reveal unexpected placements for fossil taxa. *PLoS ONE* **10:** e0118199. doi: 10.1371/journal.pone.0118199

Rieppel O. 1978. A functional and phylogenetic interpretation of the skull of the Erycinae (Reptilia, Serpentes). *Journal of Zoology* **186:** 185–208.

Rieppel O. 1979. The evolution of the basicranium in the Henophidia (Reptilia: Serpentes). *Zoological Journal of the Linnean Society* **66:** 411–431.

Rieppel O. 2007. The naso-frontal joint in snakes as revealed by high-resolution X-ray computed tomography of intact and complete skulls. *Zoologischer Anzeiger* **246:** 177–191.

Savitzky AH. 1983. Coadapted character complexes among snakes: fossoriality, piscivory, and durophagy. *American Zoologist* **23:** 397–409.

Scanferla A, Bhullar B-AS. 2014. Postnatal development of the skull of *Dinilysia patagonica* (Squamata-Stem Serpentes). *The Anatomical Record* **297:** 560–573.

Scanferla A, Zaher H, Novas FE, Muizon C, Céspedes R. 2013. A new snake skull from the Paleocene of Bolivia sheds light on the evolution of macrostomatans. *PLoS ONE* **8:** e57583. doi: 10.1371/journal.pone.0057583

Scanlon JD, Lee MSY. 2011. The major clades of living snakes: morphological evolution, molecular phylogeny, and divergence dates. In: Sever DM, ed. *Reproductive biology and phylogeny of snakes*. Enfield: Science Publishers Inc, 55–95.

Schaal S. 2004. *Palaeopython fischeri* n. sp. (Serpentes: Boidae), eine Riesenschlange aus dem Eozän (MP 11) von Messel. *Courier Forschungsinstitut Senckenberg* **252:** 35–45.

Schaal S, Baszio S. 2004. *Messelophis ermannorum* n. sp., eine neue Zwergboa (Serpentes: Boidae: Tropidopheinae) aus dem Mittel-Eozän von Messel. *Courier Forschungsinstitut Senckenberg* **252:** 67–77.

Schaal S, Ziegler W. 1992. *Messel – an insight into the history of life and the earth*. Oxford: Clarendon Press.

Smith KT. 2013. New constraints on the evolution of the snake clades Ungaliophiinae, Loxocemidae and Colubridae (Serpentes), with comments on the fossil history of erycine boids in North America. *Zoologischer Anzeiger* **252:** 157–182.

Smith KT, Wuttke M. 2012. From tree to shining sea: taphonomy of the arboreal lizard *Geiseltaliellus maarius* from Messel, Germany. *Palaeobiodiversity and Palaeoenvironments* **92:** 45–65.

Smith MA, Bellairs A, Miles AEW. 1953. Observations on the premaxillary dentition of snakes with special reference to the egg-tooth. *Journal of Linnean Society, Zoology* **42:** 260–268.

Szyndlar Z, Böhme W. 1996. Redescription of *Tropidonotus atavus* von Meyer, 1855 from the upper Oligocene of Rott (Germany) and its allocation to *Rottophis* gen. nov. (Serpentes, Boidae). *Palaeontographica A* **240:** 145–161.

Szyndlar Z, Rage J-C. 2003. *Non-erycine Booidea from the Oligocene and Miocene of Europe*. Krakow: Polish Academy of Sciences.

Tchernov E, Rieppel O, Zaher H, Polcyn MJ, Jacobs IJ. 2000. A new fossil snake with limbs. *Science* **287:** 2010–2012.

Thompson JD, Gibson TJ, Plewniak F, Jeanmougin F. 1997. The Clustal windows interface: flexible strategies for multiple sequence alignment aided by quality analysis tools. *Nucleic Acids Research* **25:** 4876–4882.

Vidal N, Hedges SB. 2002. Higher-level relationships of snakes inferred from four nuclear and mitochondrial genes. *Comptes Rendus Biologies* **325:** 977–985.

Vidal N, Delmas AS, Hedges SB. 2007. The higher-level relationships of alethinophidian snakes inferred from seven nuclear and mitochondrial genes. In: Henderson RW, Powell R, eds. *Biology of the Boas and Pythons*. Eagle Mountain: Eagle Mountain Publishing, 27–33.

Vinther J, Briggs DEG, Clarke J, Mayr G, Prum RO. 2010. Structural coloration in a fossil feather. *Biology Letters* **6:** 128–131.

Wake MH. 1993. The skull as a locomotor organ. In: Hanken J, Hall BK, eds. *The skull, Vol. 3*. Chicago: University of Chicago Press, 197–240.

Wiens JJ, Kuczynski CA, Smith DG, Mulcahy DG, Sites JW, Townsend T, Reeder TW. 2008. Branch length, support, and congruence: testing the phylogenomic approach with 20 nuclear loci in snakes. *Systematic Biology* **57:** 420–431.

Wiens JJ, Kuczynski CA, Townsend T, Reeder TW, Mulcahy DG, Sites W. 2010. Combining phylogenomics and fossils in higher-level squamate reptile phylogeny: molecular data change the placement of fossil taxa. *Systematic Biology* **59:** 674–688.

Wiens JJ, Hutter CR, Mulcahy DG, Noonan BP, Townsend TM, Sites JW, Reeder TW. 2012. Resolving the phylogeny of lizards and snakes (Squamata) with extensive sampling of genes and species. *Biology Letters* **8:** 1043–1046.

Wilcox TP, Zwickl DJ, Heath TA, Hillis DM. 2002. Phylogenetic relationships of the dwarf boas and a comparison of Bayesian and bootstrap measures of phylogenetic support. *Molecular Phylogenetics and Evolution* **25:** 361–371.

Wilson JA, Mohabey D, Peters S, Head JJ. 2010. Predation upon hatchling sauropod dinosaurs by a new basal snake from the Late Cretaceous of India. *PLoS Biology* **8:** e1000322.

Wuttke M. 1983. Weichteilerhaltung durch lithifizierte Mikroorganismen bei mitteleozänen Vertebraten aus den Ölschiefern der Grube Messel bei Darmstadt. *Senckenbergiana Lethaea* **64:** 509–527.

Zaher H. 1994. Les Tropidopheoidea (Serpentes; Alethinophidia) sont-ils réellement monophylétiques? Arguments en faveur de leur polyphylétisme. *Comptes Rendus Academie des Sciences (Sciences de la vie)* **317:** 471–478.

SUPPORTING INFORMATION

Additional supporting information may be found in the online version of this article at the publisher's web-site:

Appendix S1. Details of phylogenetic analyses and specimens examined.